

Signatures of a localizable bath in the memory kernel of a generalized quantum master equation

Nathan Ng¹ and Eran Rabani^{2,3,4}

¹*Department of Physics, University of California, Berkeley, CA 94720, USA*

²*Department of Chemistry, University of California, Berkeley, CA 94720, USA*

³*Materials Sciences Division, Lawrence Berkeley National Laboratory, Berkeley, CA 94720, USA*

⁴*The Sackler Center for Computational Molecular and Materials Science, Tel Aviv University, Tel Aviv 69978, Israel*

(Dated: May 27, 2022)

We study the properties of the Nakajima-Zwanzig memory kernel for a qubit immersed in a many-body localized (i.e. disordered and interacting) bath. We argue that the memory kernel decays as a power law in both the localized and ergodic regimes, and show how this can be leveraged to extract $t \rightarrow \infty$ populations for the qubit from finite time ($Jt \leq 10^2$) data in the thermalizing phase. This allows us to quantify how the long time values of the populations approach the expected thermalized state as the bath approaches the thermodynamic limit. This approach should provide a good complement to state-of-the-art numerical methods, for which the long-time dynamics with large baths are impossible to simulate in this phase. Additionally, our numerics on finite baths reveal the possibility for long-time unbounded exponential growth in the memory kernel, a phenomenon rooted in the appearance of exceptional points in the projected Liouvillian governing the reduced dynamics. This behavior, while pathological, may have interesting connections to localization and the validity of perturbative expansions of the memory kernel.

Central spin models are ubiquitous in physical and chemical settings, from electrons with hyperfine coupling to nuclear spins inside quantum dots [1–4], to nitrogen-vacancy centers in diamond [5–7]. Depending on the couplings in these systems, the central spin may have long-lived, slow decaying dynamics suitable for quantum information applications. The role of the bath in these cases is relegated to modelling decoherence, and has not traditionally been considered to be important. The bath is usually taken to be non-interacting, an assumption which has proven fruitful in the development of analytical [8–14] and numerical [15–20] techniques. As such, these classes of baths – whether composed of bosons [21] or spins [22] – are by now reasonably well understood [22–30].

Recent research has brought new focus to modifications of the bath by adding, for example, intra-bath interactions and disorder. With these additions, the bath alone can exhibit novel dynamical phases such as many-body localization (MBL), which serves as a basis for non-ergodicity in generic systems with strong disorder. Upon coupling to a bath, the long-ranged mediated interactions between constituents of the bath can push the bath towards delocalization. Recent work [31, 32] has shown that a single qubit coupled centrally to a 1D MBL spin chain can preserve localization provided that the magnitude of the central coupling decays fast enough with the size of the bath. But generally in these types of models, analytical and numerical approaches become scant due to the presence of interactions in the bath and to the star-like geometry of problem.

The added complexity has a drawback in that such systems quickly become intractable computationally, even for small bath sizes of $\sim O(30)$ degrees of freedom. This is due to the exponential increase of states in the Hilbert space that are involved in the dynamics. Moreover, large intra-bath interactions and disorder can radically change

the timescales of the bath and invalidate perturbative approaches to bath dynamics. In this context, the case of MBL (in one dimension) is special in that it allows for a non-perturbative description in terms of ‘l-bits’ [33–36]. Owing to this and to the slow growth of entanglement entropy [37, 38], dynamics in the localized phase of MBL systems are by now well explored numerically and analytically [36, 39–42]; however, these approaches generally fail on the ergodic side of the transition.

The dynamics of extended, thermalizing many-body systems are typically very difficult to simulate exactly due to the rapid growth of entanglement. This is, for example, the limiting factor in methods based on a tensor network ansatz for the wavefunction in which the bond dimension bounds the amount of entanglement entropy that can be captured. A reasonable strategy then would be to extend the timescale of the converged simulation using information that can be computed on the timescales before the breakdown of the numerical method. Such an approach had been used successfully in the past to find the steady state behavior of quantum impurity systems [43–45], and to show the existence of bistability in the Anderson-Holstein model [46]. In those applications, the nontrivial dynamics of the impurity could be described exactly using a memory kernel, derived using the projection operator formalism described by Mori and Zwanzig [47, 48].

While the Mori-Zwanzig theory is formally exact, it is oftentimes more demanding than other formalisms to describe the dynamics because of the time-nonlocal memory kernel that naturally arises in their approach. It only becomes computationally useful if the nonlocality can be restricted, e.g. large timescale separation between bath and system dynamics lending to Markovian approximations, or if memory kernel decays sufficiently rapidly such that it can be truncated for times $\geq t_c$, where t_c is the

cutoff time.

In this paper we study the memory kernel of a two-level system immersed in a bath modelled by a many-body localizable spin chain. We do so with two goals in mind: to assess the feasibility of extending the system dynamics from short time calculations when analytical and direct numerical approaches to compute the system dynamics fail (i.e. on the thermalizing side of the MBL transition); and to understand how interactions and disorder in the bath affect the memory kernel in properties such as timescales and tail behavior.

To this end, we will work with a previously studied model [31] of a qubit ($\hat{\tau}^{x,y,z}$) coupled to a disordered Heisenberg chain of L spins-1/2 ($\hat{\sigma}_i^{x,y,z}$):

$$\begin{aligned}\hat{H} &= \hat{H}_S + \hat{H}_B + \hat{V}, & \hat{H}_S &= \Omega \hat{\tau}^z \\ \hat{H}_B &= \sum_{i=1}^L J_z \hat{\sigma}_i^z \hat{\sigma}_{i+1}^z + J_\perp (\hat{\sigma}_i^+ \hat{\sigma}_{i+1}^- + \text{h.c.}) + \frac{h_i}{2} \hat{\sigma}_i^z \\ \hat{V} &= \frac{1}{L} \sum_{i=1}^L \gamma_z \hat{\sigma}_i^z \hat{\tau}^z + \gamma_\perp (\hat{\sigma}_i^+ \hat{\tau}^- + \text{h.c.})\end{aligned}\quad (1)$$

where the $\hat{\tau}$ and $\hat{\sigma}$ are Pauli matrices. The bath Hamiltonian \hat{H}_B has parameters corresponding to the isotropic Heisenberg chain, $J_z = J/4$, $J_\perp = J/2$, where $J = 1$. The system-bath coupling terms \hat{V} are likewise given by the Heisenberg interaction such that $\gamma_z = \gamma/4$, $\gamma_\perp = \gamma/2$. Finally, as was done by Ref. [31], the magnetic field is set to $\Omega = 0$. The strength of the central coupling is controlled by the γ . The random longitudinal fields h_i are drawn independently and uniformly from $[-W, W]$. In the high frequency limit where $\Omega \gg L$, the intrinsic dynamics of the central qubit will be so fast that its dynamics effectively decouples from that of the bath's. Localization in this limit is independent of the qubit, and is dictated by MBL physics. We focus on the other extreme, where the qubit has no intrinsic dynamics and is instead entirely dependent on the magnitude of the Overhauser field it experiences from the bath.

The structure of this paper is as follows: we shall first define the memory kernel for reduced dynamics and consider the role of disorder averaging; then we shall analyze the physics underlying the memory kernel at short, intermediate, and long times; and finally we shall discuss the potential for the memory to be used to augment short-time experimental or numerical data.

I. THE NAKAJIMA-ZWANZIG EQUATION

We quickly review the basics of the projection operator approach to generalized quantum master equations. Any given Hamiltonian can be split into contributions \hat{H}_S acting only on the system. \hat{H}_B acting only on the bath, and \hat{V} coupling the two. To each of these operators is associated a corresponding Liouvillian superoperator ($\mathbb{L}_S \cdot \equiv [\hat{H}_S, \cdot]$, $\mathbb{L}_B \cdot \equiv [\hat{H}_B, \cdot]$, $\mathbb{L}_V \cdot \equiv [\hat{V}, \cdot]$) generating

dynamics for the density matrix

$$i \frac{d\hat{\rho}}{dt} = i \frac{d}{dt} e^{-i\mathbb{L}t} \hat{\rho}_0 = \mathbb{L} \hat{\rho}(t) \equiv (\mathbb{L}_S + \mathbb{L}_B + \mathbb{L}_V) \hat{\rho}(t). \quad (2)$$

Oftentimes one is interested only in the dynamics of the system, in which case the bath degrees of freedom can be projected out by tracing over the bath on both sides of the equation, where the bath trace is

$$\text{Tr}_B \hat{O} = \sum_{s,s'}^{\dim \mathcal{H}_S \dim \mathcal{H}_B} |s\rangle \langle s'| \langle s \otimes b | \hat{O} | s' \otimes b \rangle. \quad (3)$$

This is used to define the system reduced density matrix,

$$\hat{\rho}_S(t) = \text{Tr}_B \hat{\rho}(t). \quad (4)$$

We shall additionally assume that the initial state is factorized, i.e. $\hat{\rho}_0 = \hat{\rho}_{S,0} \otimes \hat{\rho}_B$. By taking the bath trace defined in Eq. (3) on both sides of Eq. (2) and using $\text{Tr}_B \mathbb{L}_B = 0$, we arrive at the exact expression

$$i \frac{d}{dt} \hat{\rho}_S(t) = \mathbb{L}_S \hat{\rho}_S(t) + \text{Tr}_B (\mathbb{L}_V e^{-i\mathbb{L}t} (\hat{\rho}_{S,0} \otimes \hat{\rho}_B)), \quad (5)$$

which is an equation of motion for $\hat{\rho}_S(t)$ that explicitly depends on knowledge of the time evolution of the full system and bath. This equation of motion can be closed, i.e. involving only $\hat{\rho}_S(t)$, by using Dyson's identity (see [47, 49]):

$$i \frac{d}{dt} \hat{\rho}_S(t) = \mathbb{L}_S \hat{\rho}_S(t) - \int_0^t d\tau \mathbb{K}(t - \tau) \hat{\rho}_S(\tau). \quad (6)$$

The memory kernel superoperator is formally defined as

$$\mathbb{K}(t) \hat{\rho}_S = \text{Tr}_B (\mathbb{P} \mathbb{L} \mathbb{Q} e^{-i\mathbb{L} \mathbb{Q} t} \mathbb{Q} \mathbb{L} \hat{\rho}_S \otimes \hat{\rho}_B). \quad (7)$$

In the above equation, the projection superoperator is taken to be $\mathbb{P} \cdot \equiv \text{Tr}_B(\cdot) \otimes \rho_B$ and $\mathbb{Q} = \mathbb{I} - \mathbb{P}$ is its complement. It is useful to define the system reduced propagator (superoperator) such that

$$\mathbb{U}_S(t) \hat{\rho}_{S,0} \equiv \hat{\rho}_S(t) = \text{Tr}_B (e^{-i\mathbb{L}t} \hat{\rho}_{S,0} \otimes \hat{\rho}_B). \quad (8)$$

Knowledge of \mathbb{U}_S allows for the generation of $\hat{\rho}_S(t)$, and lets us write a Nakajima-Zwanzig equation [50] involving only objects of one type, i.e. superoperators:

$$\frac{d}{dt} \mathbb{U}_S(t) = -i \mathbb{L}_S \mathbb{U}_S(t) - \int_0^t dt' \mathbb{K}(t - t') \mathbb{U}_S(t'), \quad (9)$$

In this form, it becomes clear that one can solve for \mathbb{K} directly from \mathbb{U}_S . Note that no approximations have been made and the dynamics generated by solving Eqs. (9) and (7) are equivalent to solving Eq. (2) with the stated assumptions on initial conditions.

The derivation however, benefits from a simplification made possible by the form of the model Hamiltonian in Eq. (1). Bath traces over the interaction Liouvillian \mathbb{L}_V with respect to a bath state $\hat{\rho}_B$ of fixed magnetization will

be zero due to the conservation of total magnetization in the model, and if we choose ρ_B to have zero magnetization. Therefore the validity of Eq. (7) is not restricted to solely thermal baths ($\hat{\rho}_B \propto e^{-\beta \hat{H}_B}$) nor bath eigenstates ($[\hat{\rho}_B, \hat{H}_B] = 0$).

The memory kernel \mathbb{K} and the system propagator \mathbb{U}_S , being linear mappings from the system Hilbert space \mathcal{H}_S to itself, can be represented as $(\dim \mathcal{H}_S)^2 \times (\dim \mathcal{H}_S)^2$ matrices. Requirements on unitarity and hermiticity, along with the decoupling of populations and coherences in this magnetization-conserving model, means that \mathbb{U}_S is described by only two independent entries when the focus is solely on population dynamics. The same extends to \mathbb{K} by virtue of its relation to \mathbb{U}_S . The two entries of \mathbb{U}_S are computed by two independent instances of the initial system state $\rho_{S,0}$: one from the population of the $|0\rangle$ state when $\rho_{S,0} = |0\rangle\langle 0|$, and the other from the population of the $|1\rangle$ state when $\rho_{S,0} = |1\rangle\langle 1|$. The initial bath state is the same in both cases, with definite magnetization $M_B = 0$. Because the total magnetization $\hat{M}^z = \hat{\tau}^z + \sum_i \hat{\sigma}_i^z$ is conserved, these two trajectories must reside in independent parts of Hilbert space. They are then combined in solving for the memory kernel, which can be done in the time domain by discretizing the integro-differential equation (see appendix for details). This, while posing no problem for the projection operator formalism, leads to a strange scenario where the central spin dynamics restricted to one symmetry sector will depend on information from another, disjoint symmetry sector.

To skirt around this unsavory philosophical scenario, we can focus on only the population of the $|0\rangle$ state of the central spin. Using the projection operator $\mathbb{P}\hat{\rho} = (|0\rangle\langle 0| \otimes \hat{\rho}_B) \text{Tr}[(|0\rangle\langle 0| \otimes \hat{I}_B)\hat{\rho}]$, we have the scalar memory kernel for a single disorder realization as

$$K(t) = \text{Tr} \left[(|0\rangle\langle 0| \otimes \hat{I}_B) \mathbb{L} Q e^{-i\mathbb{L} Q t} \mathbb{L} (|0\rangle\langle 0| \otimes \hat{\rho}_B) \right], \quad (10)$$

satisfying the integro-differential equation

$$\frac{d}{dt} p_0(t) = - \int_0^t dt' K(t-t') p_0(t'), \quad (11)$$

or its Laplace-domain equivalent

$$\tilde{K}(z) = -z + \frac{1}{\tilde{p}_0(z)}. \quad (12)$$

Focusing on the population $p_0(t)$ of single state allows us to work with a scalar memory kernel $K(t)$ and simplifies the calculations. We will focus exclusively on the scalar memory kernel for the remainder of this paper.

Note that the memory kernel is akin to the self-energy for the reduced density matrix. Solving for it is then tantamount to solving the exact problem. Yet there are still advantages to working with the memory. For one, because of its relationship with the central spin's populations it is in principle a measurable quantity. There is

also the possibility for the memory to decay on timescales different from that of the populations. Should the memory decay much faster, then it may be possible to leverage the timescale separation to reduce the computational effort required to solve for the system dynamics at longer times.

II. DISORDER AVERAGED MEMORY

Given that we are interested in disordered systems, suitable definitions of a memory kernel associated with different disorder realizations depends on the quantity of experimental interest. The difference depends on when the disorder averaging is performed. We denote by K_{avg} the case where the population p_0 is averaged over the disorder (\bar{p}_0) before solving for the memory kernel, satisfying

$$\frac{d}{dt} \bar{p}_0(t) = - \int_0^t dt' K_{\text{avg}}(t-t') \bar{p}_0(t'). \quad (13)$$

The other case, where the memory for disorder realization is found and then averaged, is denoted by \bar{K} . This latter case is relevant should one decide that the observable of interest is the memory kernel itself, which is in principle possible since it is directly computable from the populations.

It is not *a priori* clear how these two definitions are related. A reasonable guess might be that, upon disorder averaging, the two definitions are equivalent. We argue that this is not necessarily correct. Suppose that for every L the disorder-averaged population $\bar{p}_0(t)$ exists, with initial condition $\bar{p}_0(0) = 1$. The trajectory of the population for a single instance of disorder will have deviations from this average value, $p_0(t) = \bar{p}_0(t) + \delta p(t)$. Since populations must be positive at all times, so should their Laplace transforms for real, positive z . Using Eq. (12), the positivity of the Laplace transforms allows us to write

$$\begin{aligned} \widetilde{\delta K}(z) &= \frac{1}{\tilde{p}_0(z) + \widetilde{\delta p}(z)} - \frac{1}{\tilde{p}_0(z)} \\ &= \int_0^\infty du e^{-u(\tilde{p}_0(z) + \widetilde{\delta p}(z))} - e^{-u\tilde{p}_0(z)} \\ &= \int_0^\infty du e^{-u\tilde{p}_0(z)} \left(e^{-u\widetilde{\delta p}(z)} - 1 \right). \end{aligned} \quad (14)$$

Since the exponential function is entire, the term in parentheses can be expanded as a series,

$$\widetilde{\delta K}(z) = \int_0^\infty du e^{-u\tilde{p}_0(z)} \sum_{n=1}^\infty \frac{(-u)^n}{n!} \left(\widetilde{\delta p}(z) \right)^n. \quad (15)$$

Averaging this expression over disorder, we will have the $n = 1$ term vanish by definition of δp . But all higher order terms – particularly ones with even powers – are not guaranteed to vanish. The consequence is that $K_{\text{avg}} \neq \bar{K}$ for finite L .

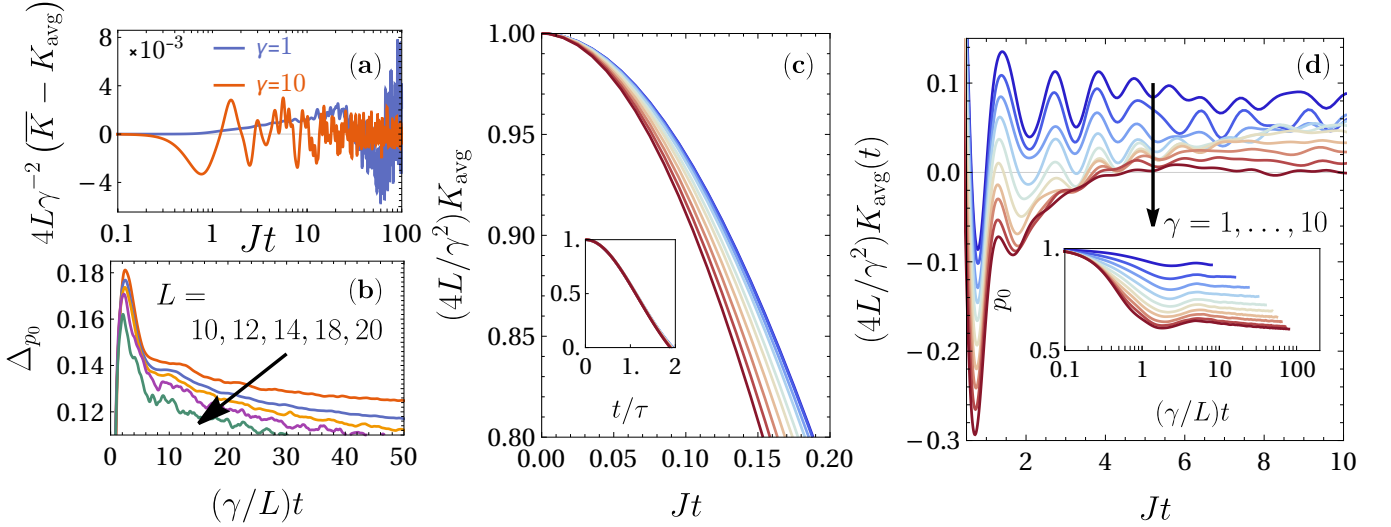


FIG. 1. (a) Comparison of the averaged memory kernel \bar{K} and the memory kernel of the average K_{avg} for $L = 16$ deeply in the localizing ($\gamma = 1$) and thermalizing ($\gamma = 10$) phases, with ≥ 500 disorder realizations. (b) Root-mean-squared fluctuations Δp_0 of the population for $\gamma = 10$. (c,d) The scalar memory kernel of the averaged population, $K_{\text{avg}}(t)$, for $L = 12$, onsite disorder strength $W = 6.0$, and with 6400 disorder realizations. The memory is rescaled such that its initial value is 1, and separated into the (c) short and (d) intermediate time regimes. For clarity, the data in the main panel of (d) are shifted up in multiples of 0.1 away from the $\gamma = 10$ curve. (c, inset) Collapse of the short time memory upon rescaling the time by τ defined in Eq. (20). (d, inset) The populations of the $|0\rangle$ state for the central spin used to generate K_{avg} .

The situation is modified in the thermodynamic limit owing to the phenomenon of self-averaging/dynamical typicality. Intuitively, a small subsystem interacting randomly with $N \gg 1$ degrees of freedom should have deviations from its mean behavior that decrease as N increases. As a result, when the environment is sufficiently large, a single realization of the random interaction should typically yield results close to the mean. This statement was recently demonstrated [51], showing that the system reduced density matrix enjoys the typicality property for system-bath interactions modelled by certain classes of random matrices. More concretely, they had shown that the reduced density matrix of the system at time t ,

$$\hat{\rho}_{S,t}(\hat{V}) = \text{Tr}_B \left[e^{-i(\hat{H}_S + \hat{H}_B + \hat{V})t} \hat{\rho}(0) e^{i(\hat{H}_S + \hat{H}_B + \hat{V})t} \right], \quad (16)$$

for a single realization of the random interaction \hat{V} has typical deviations from the average (performed over all \hat{V}) bounded by $\lesssim t^{1/2}(\dim \mathcal{H}_B)^{-1/2}$, the size of the Hilbert space of the bath [52]. This bound becomes exponentially small in L , the number of sites of the bath, as $L \rightarrow \infty$. Importantly, their work does not make assumptions about the microscopic details of the bath, e.g. the same bounds hold regardless of the initial bath state or whether the bath can localize. While the model we consider has a random \hat{H}_B instead of a random interaction, it should be possible to map Eq. (1) to an equivalent model in which the randomness resides in the qubit-spin interaction. Specifically, we can make a one-to-one correspondence between a bath spin state in the z -basis to the presence (\bullet) or absence (\circ) of kinks between a bath

spin and the central qubit, i.e.

$$\begin{aligned} |0\rangle \otimes |\uparrow\rangle &\Leftrightarrow |0\rangle \otimes |\bullet\rangle & |0\rangle \otimes |\downarrow\rangle &\Leftrightarrow |0\rangle \otimes |\circ\rangle \\ |1\rangle \otimes |\uparrow\rangle &\Leftrightarrow |0\rangle \otimes |\circ\rangle & |1\rangle \otimes |\downarrow\rangle &\Leftrightarrow |1\rangle \otimes |\bullet\rangle \end{aligned}$$

In terms of operators, this is tantamount to making the substitutions,

$$\begin{aligned} \hat{\sigma}_i^x &= \hat{\mu}_i^x & \hat{\sigma}_i^y &= \hat{\tau}^z \hat{\mu}_i^y & \hat{\sigma}_i^z &= \hat{\tau}^z \hat{\mu}_i^z \\ \hat{\tau}^+ \hat{\sigma}_i^- &= \hat{\tau}^+ \prod_{j \neq i} \hat{\mu}_j^x, \end{aligned} \quad (17)$$

where the $\hat{\mu}^{x,y,z}$ follow the usual Pauli commutation relations. With this transformation, the Hamiltonian becomes

$$\begin{aligned} \hat{H}' &= \Omega \hat{\tau}^z + \sum_{i=1}^L \frac{\Delta}{4} \hat{\mu}_i^z \hat{\mu}_{i+1}^z + \frac{\hat{\mu}_i^+ \hat{\mu}_{i+1}^- + \text{h.c.}}{2} + \frac{\gamma}{4L} \hat{\mu}_i^z \\ &+ \sum_{i=1}^L h_i \hat{\tau}^z \hat{\mu}_i^z + \frac{\gamma}{2L} (\hat{\tau}^+ + \hat{\tau}^-) \prod_{j \neq i} \hat{\mu}_j^x, \end{aligned} \quad (18)$$

with the terms on the second line now having the form of a random interaction Hamiltonian [53]. While this random interaction does not conform to the random matrices considered by Ref. [51], it is not unreasonable to assume that the basic principle underlying their proof – that of measure concentration – might still hold. But because this random interaction only depends on L random variables instead of $\dim \mathcal{H} \sim e^L$ random variables, one would expect the deviations of individual disorder realizations $p_0(t)$ from the mean $\bar{p}_0(t)$ to decay sub-exponentially

with L . In Fig. 1b we show the root-mean-squared fluctuations of $p_0(t)$ deeply in the thermalizing phase of the bath-disordered Hamiltonian (1), and observe that they indeed decrease with increasing bath size. Extrapolating to the thermodynamic limit, we should therefore have self-averaging of the reduced density matrix of the central qubit. Then by extension the memory must self-average too, since it is directly computed from the reduced density matrix. This can be seen from Eq. (15), where fluctuations of a single realization of $K(t)$ has deviations from $K_{\text{avg}}(t)$ that are bounded by the magnitude of the fluctuations in the population $\delta p(t) = p_0(t) - \overline{p_0}(t)$. In Fig. 1a, we find that $\overline{K}(t)$ and $K_{\text{avg}}(t)$ generally tend to differ by $|\overline{K}(t) - K_{\text{avg}}(t)| \sim O(10^{-3}(\gamma^2/4L))$ up to timescales $t \lesssim O(10^2)$ for the system sizes we can simulate. We observe that this deviation can diverge exponentially with a finite number of disorder realizations at long enough times, a phenomenon which we will return to in Sec. III C. Barring that, the self-averageness of the population $p_0(t)$ – which yields the equivalence $\overline{K}(t) = K_{\text{avg}}(t)$ in the thermodynamic limit – gives us an alternate window into understanding how the memory kernel behaves. For the remainder of this paper, we shall mostly discuss $K_{\text{avg}}(t)$ as we are interested also in the dynamics of the averaged population.

III. RESULTS FOR INTERACTING BATH

We implement time evolution by approximating $e^{-i\hat{H}t}$ with Chebyshev polynomials [54, 55]. To reduce computational costs, we use the conservation of total magnetization $\hat{M}^z = \hat{\tau}^z + \sum_i \hat{\sigma}_i^z$ in the model, allowing us to restrict the dynamics to the symmetry sector with $\hat{M}^z = -1$. The system is prepared in the $\hat{\rho}_{S,0} = |0\rangle\langle 0|$ state, while the bath state $\hat{\rho}_B$ is initialized to be a Neel state, $|\cdots \downarrow \uparrow \downarrow \uparrow \cdots\rangle$. We expect similar results should we choose different initial states within the sector of $\hat{M}^z = -1$.

A (matrix) memory kernel \mathbb{K} with n independent entries can be computed directly from the populations [50] using n different initial conditions, for each disorder realization. In this sense, there is added computational benefit to restricting our discussion to only the scalar memory kernel $K(t)$.

A. Short times

We can leverage the self-averaging property to gain some understanding of the short time behavior (Fig. 1c) of $K_{\text{avg}}(t)$. The derivatives of $K(t)$ at $t = 0$ for a single disorder realization can be found straightforwardly from those of $p_0(t)$, with the lowest orders being

$$\begin{aligned} K(t=0) &= -p_0^{(2)}(t=0) \\ K^{(2)}(t=0) &= -p_0^{(4)}(t=0) + \left(p_0^{(2)}(t=0)\right)^2, \end{aligned} \quad (19)$$

where $f^{(n)}$ denotes the n -th derivative. After averaging over disorder with an initial Neel state in the bath, we have

$$\begin{aligned} \frac{K_{\text{avg}}(t)}{\gamma^2/4L} &\approx 1 - \frac{1}{2} \left(\frac{t}{\tau_K}\right)^2 + O(t^4) \\ \frac{1}{\tau_K} &\equiv \sqrt{\frac{W^2}{3} + \frac{3J}{4} \frac{\gamma}{L} + \frac{3}{4} \frac{\gamma^2}{L} - \frac{3}{4} \frac{\gamma^2}{L^2}}, \end{aligned} \quad (20)$$

where $J = 1$ in our model, and L is the number of spins in the bath. We see that the disorder strength W sets the initial decay rate $1/\tau_K$. This can be roughly estimated for large W from Fermi's Golden Rule, using our argument that disorder-averaging effectively gives us a continuous spectrum with an effective (root-mean-squared) bandwidth $\sim O(W\sqrt{L})$, and a coupling strength $\sim (\gamma_\perp/L)^2 = \gamma^2/4L^2$. While W sets the decay timescale for $K_{\text{avg}}(t)$, it is the quantity $\gamma^2/4L$ that sets the overall magnitude of $K_{\text{avg}}(t)$ and so dictates the timescale for $p_0(t)$. We expect so from the following scaling argument: Assume that the memory kernel converges to a limiting form in the thermodynamic limit as

$$\lim_{L \rightarrow \infty} \frac{K_{\text{avg}}(t)}{\gamma^2/4L} = k(t), \quad (21)$$

where $k(t)$ is independent of L and has a short time expansion given by Eq. (20). From the Nakajima-Zwanzig equation,

$$\frac{dp_0}{dt} \approx -\frac{\gamma^2}{4L} \int_0^t d\tau k(\tau) p_0(t-\tau), \quad (22)$$

we rescale the time to $t' = (\gamma^r/L^s)t$ and obtain

$$\frac{dp'_0}{dt'} = -\frac{\gamma^{2-2r}L^{2s-1}}{4} \int_0^{t'} d\tau' k\left(\frac{L^s\tau'}{\gamma^r}\right) p'_0(t' - \tau'), \quad (23)$$

where $p'_0(t') \equiv p_0(t'/(\gamma^r L^{-s}))$. We seek exponents $r > 0$ and $s > 0$ such that $p'_0(t')$ will vary on the timescale $\Delta t' \sim 1$. With the rescaled time, the $k(L^s\tau'/\gamma^r)$ appearing in Eq. (23) will have largely decayed by $\tau' \sim \gamma^r L^{-s}/(W/\sqrt{3})$, a timescale much faster than that of $p'_0(t')$. Hence we can approximate $p'_0(t' - \tau')$ in Eq. (23) as a constant, and estimate the strength of memory effects by integrating $k(L^s\tau'/\gamma^r)$ up to its decay time. This is roughly given by

$$\left(\frac{\gamma^{2-2r}L^{2s-1}}{4}\right) \left(\frac{\gamma^r/L^s}{W/\sqrt{3}}\right) = \frac{\sqrt{3}}{4} \frac{\gamma^{2-r}}{W} L^{s-1}. \quad (24)$$

We require $s = 1$ in order to have a converged p'_0 on the timescale of t' in the thermodynamic limit. Furthermore, $r = 1$ so that a trivial rescaling of the Hamiltonian $\hat{H} \rightarrow \alpha \hat{H}$ would not alter the strength of the memory term. Thus we argue that the dynamics of the central spin should proceed on the timescale $\tau_{p_0} \sim L/\gamma$, consistent with our initial assumption that the population

dynamics proceed much more slowly than does its associated memory kernel. We show this rescaling of time in Fig. 1b and in the inset of Fig. 1d, where the former shows the fluctuations of $p_0(t)$ between disorder realizations for different system sizes at fixed $\gamma = 10$, and the latter shows $p_0(t)$ for fixed $L = 12$ across γ . These figures show that the lowest moments of the populations align on the timescale $\tau_{p_0} \sim L/\gamma$. This result is also consistent with the result of [31] on the central spin's autocorrelation function, $\langle \hat{\tau}^z(t + \tau) \hat{\tau}^z(\tau) \rangle$, where it was observed that there is an accumulation of spectral weight near $\omega \sim \gamma/L$.

With a clear separation between τ_K and τ_{p_0} , one may wonder whether the central qubit can be described by an effective master equation. At least deep in the localized phase, the bath is too slow to act as an effective reservoir for the central system. Correlation functions of the bath are argued [56, 57] to decay as a power law $t^{-\zeta}$ with $0 < \zeta < 1$, which makes memory effects crucial in dictating the behavior of $p_0(t)$ at long times. We will return to discuss the long time behavior of the memory kernel below in Sec. III C.

B. Intermediate times

As seen in Fig. 1d, the memory past $Jt \gtrsim 1$ takes on different behaviors depending on the coupling strength, with increasingly damped oscillations as the combined system and bath transitions from localization to thermalization. The inset of Fig. 1d shows that this behavior is not observable when looking solely at the populations. The oscillation is dominated by frequencies in the range $\omega \in (4, 6)$, close to the disorder strength $W = 6$. Such oscillations are not a feature unique to an interacting bath. They show up in the non-interacting limit $J_\perp = J_z = 0$, in which the memory to lowest order in γ can be approximated by

$$K_{J_\perp=J_z=0}(t) \approx \frac{\gamma_\perp^2}{L} \frac{\sin(Wt)}{Wt} + O(\gamma^3). \quad (25)$$

We see that oscillations are linked to the finite bandwidth W of frequencies in the bath [43], which arises from precession about the local field on each site, $(h_i/2)\hat{\sigma}_i^z$, and $h_i \in [-W, W]$. When interactions in the bath are turned on, we would expect them to provide a small renormalization to the precession frequencies, as we are working with a hierarchy of scales such that $W \gg J_\perp, J_z > \gamma_\perp, \gamma_z$. This assumes, of course, that the bath dynamics are approximately describable with a precession picture even in the presence of bath interactions.

To justify this picture more formally, we can leverage the description of MBL systems in terms of quasi-local integrals of motion, which form the effective bath degrees of freedom that exhibit precession. At intermediate times and at weak coupling, the memory kernel can be approx-

imated by bath correlation functions [48, 58],

$$K(t) \approx \frac{\gamma_\perp^2}{L^2} \sum_{i,j} \text{Tr} [\hat{\sigma}_i^\pm(t) \hat{\sigma}_j^\mp(0) \hat{\rho}_B]. \quad (26)$$

In the MBL phase, the bath spin operators $\hat{\sigma}_i^\pm$ have large overlaps [33] with quasi-local operators $\hat{\Theta}_i^{x,y,z}$ with which the bath Hamiltonian can be written as [33, 35, 57]

$$\hat{H}_B = \sum_{i=1}^L \varepsilon_i \hat{\Theta}_i^z + \sum_{i,j} J_{i,j} \hat{\Theta}_i^z \hat{\Theta}_j^z + \dots, \quad (27)$$

where the operators $\hat{\Theta}_i^{x,y,z}$ follow the Pauli commutation relations. The bath correlation functions oscillate according to ε_i , at least when the bath is strongly localized. The distribution of ε_i will therefore set the frequency of intermediate-time oscillations in the memory kernel. We note that the couplings in Eq. (27) can be extracted directly [59, 60] from the bath Hamiltonian. Eq. (27) makes clear also that the picture of precessions is complicated at later times by dephasing mechanisms arising from interactions – the 2-body $J_{i,j}$ terms and higher – in the bath.

At the other extreme, where the system strongly couples ($\gamma \gtrsim 5$ for the value of $W = 6$ we have shown in Fig. 1d) to the bath, the locality inherent in the above picture breaks down [32]. Furthermore, the bath interactions mediated by the qubit are strong enough that the bath cannot remain “close” to its initial state, so the expansion of the memory in terms of bath correlation functions no longer holds. In all, the contribution of the bath to the system dynamics can no longer be parsed into contributions from (nearly) independent oscillators. Instead, delocalization evidently serves to homogenize the influence of the bath, smoothing over the randomness from the local fields h_i , and damping out oscillations in $K_{\text{avg}}(t)$ as observed in the red curves of Fig. 1d. Assuming the above behaviors deeply in the localized and delocalized phases hold true in the thermodynamic limit, it may be possible to correlate the presence of oscillations at finite times to MBL.

C. Long times

Within the particular parameters we have chosen to study in this model, we define “long times” to correspond to $Jt \gtrsim 10$, a time past which the coherent oscillations in the bath have dephased. For the purpose of extrapolating the dynamics, it is crucial to understand how quickly $K_{\text{avg}}(t)$ decays, if it even does so at all. It should be pointed out that, strictly speaking, the memory cannot decay to zero as $t \rightarrow \infty$ for finite systems due to the finitude of the recurrence time τ_R [47], which increases exponentially with the size of the Hilbert space [61]. The recurrence time is rooted in the small but nonzero energy level spacing in finite systems. By disorder averaging

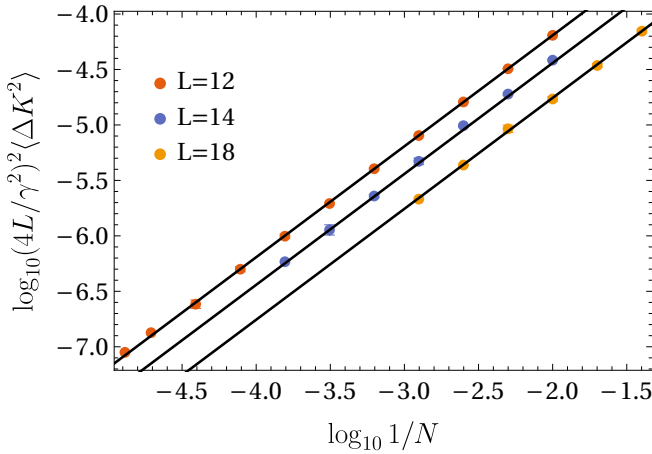


FIG. 2. Average squared deviations on $t \in [50, 100]$ of $K_{\text{avg}}(t)$ in the thermalizing regime ($\gamma = 10$), as a function of disorder realizations N . Solid lines denote $1/N$ decay and serve as guides to the eye.

the populations, we artificially “fill in” the gaps in the energy spectrum that dictate $1/\tau_R$, and argue therefore that we will not need to worry about recurrent behaviors as $t \rightarrow \infty$. Indeed, disorder averaging the dynamics can be thought of as introducing dissipation [62], under which recurrences cannot occur [63]. However, since we can only numerically average over a finite number N of disorder realizations, we cannot expect to observe a clear decay signal. Instead, we can ask whether the long time behavior of $K_{\text{avg}}(t)$ is consistent with small, possibly vanishing, values should we extrapolate our results to infinite N . Deeply in the thermalizing phase, we show in Fig. 2 that the magnitude of time-averaged fluctuations

$$\langle \Delta K^2 \rangle_{[T_i, T_f]} = \langle K_{\text{avg}}^2(t) \rangle_{[T_i, T_f]} - \langle K_{\text{avg}}(t) \rangle_{[T_i, T_f]}^2, \quad (28)$$

in the tail portion $K_{\text{avg}}(50 \leq t \leq 100)$ decays as $1/\sqrt{N}$, and moreover decreases with increasing system size as would be expected from self-averaging systems. In the above equation, we use the notation $\langle g(t) \rangle_{[T_i, T_f]} = \int_{T_i}^{T_f} dt g(t) / (T_f - T_i)$.

The persistence of the finite N noise makes it difficult to conclusively show numerically whether $K(t)$ decays as algebraically or exponentially. While in Sec. III A we argued for a power law decay for the weakly coupled, localized phase based on known phenomenology of MBL, this approach cannot work for the strongly coupled, thermalizing phase. In the absence of weak coupling perturbative expansions we now turn to the self-averaging relations $K_{\text{avg}} \sim K \sim \bar{K}$ to attempt to extract insights about the thermalizing phase. Doing so requires discussion about the memory kernel for a single realization of disorder, which is what we shall focus on for the remainder of this subsection.

For certain realizations of $\{h_i\}$, we observe an increasing likelihood for the memory – both scalar- and matrix-

valued versions – to display unbounded exponential divergences with increasing coupling γ . We can verify the divergence for small system sizes $L \lesssim 6$, where the Laplace transformed memory kernel can be computed directly to yield the memory as a sum over simple poles, some of which with positive real parts. Such contributions – which are necessary in order to correctly reproduce the population dynamics – lead to an unbounded exponential *increase* of the memory for particular values of the coupling and magnitude of disordered fields. We will return to discuss the origins and implications of such pathological behavior in Sec. V.

We can motivate the consequences of exponentially growing contributions to $K(t)$ by examining the structure of the poles of its Laplace transform, $\tilde{K}(z)$. Because the Hamiltonian is real and Hermitian, poles of $\tilde{K}(z)$ are given by a real polynomial (see appendix for details). The polynomial will only involve terms of even powers, z^{2n} , because $p_0(t) = p_0(-t)$. Thus if a pole s_n exists with residue r_n such that $\text{Re } s_n \neq 0$, it must be the case that poles $-s_n$, s_n^* and $-s_n^*$ must exist with residues r_n , r_n^* , and r_n^* respectively. Based on the distribution of the pole structure, any exponentially dampened part of the memory ($\text{Re } s_n < 0$) must be accompanied by an exponentially growing counterpart. We posit that in the thermodynamic limit one of two situations must hold: 1) all off-axis poles converge towards the $\text{Im } z$ axis as $L \rightarrow \infty$ to form a branch cut, or 2) some poles still exist off-axis, which because of the conjugate pairs, contributes both exponential decay and growth. In the first scenario, there are no isolated poles to cause exponential decay. In the second scenario, any exponential decay is masked by exponential growth. Moreover, even if $\text{Re } z > 0$ poles cancel upon disorder averaging, the same would happen to the $\text{Re } z < 0$ poles by virtue of the relationship between residues discussed above. Therefore we argue that even in the thermalizing phase, the memory kernel for the dynamics we have defined should not exhibit exponential decay in the limit as $L \rightarrow \infty$. This leaves open the possibility of power-law or stretched-exponential behavior, which we cannot clarify as our data is limited to finite times and finite number of disorder averages N . Finally, we reiterate the importance of the order of limits in this problem. They must be taken as

$$\lim_{t \rightarrow \infty} \lim_{L \rightarrow \infty} \lim_{N \rightarrow \infty} \quad (29)$$

to ensure that the memory kernel does not recur and to ensure the validity of the approximation $\bar{K} \approx K_{\text{avg}}$.

IV. EXTRACTING LONG TIME INFORMATION FROM THE MEMORY KERNEL

The memory kernel has a direct relation to steady state values of the reduced density matrix, provided that a steady state exists [43–46]. While the past work was done using all $d^2 \times d^2$ elements of the (matrix) memory

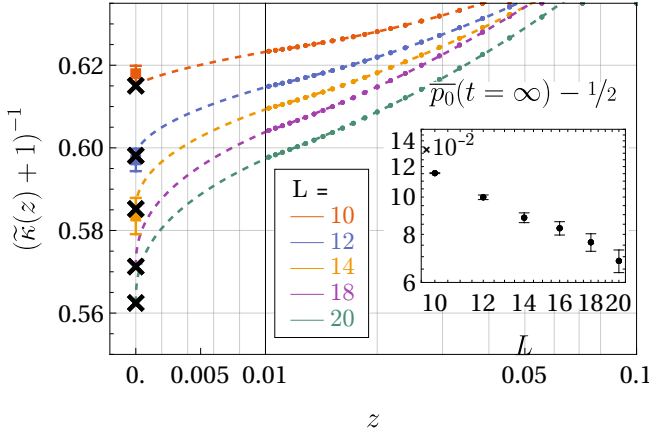


FIG. 3. Infinite time value of the average population \bar{p}_0 deeply in the thermalizing phase ($\gamma = 10$) using equations Eq. (30) and Eq. (32). Dashed lines and black crosses indicate respectively the fit to Eq. (32) and the extrapolated value for $t_c = \infty$. Where available, squares indicate the long time ($t \sim 10^{12}$) value of p_0 calculated independently from exact diagonalization. **(inset)** Log-log plot of the long time limit of \bar{p}_0 versus the number of sites in the bath, L . Error bars are obtained by varying the endpoints of the fitting interval on z .

kernel, we can import their ideas to the scalar memory kernel and a single element of the reduced density matrix. From the relationship between $\tilde{p}_0(z)$ and $\tilde{K}_{\text{avg}}(z)$, we can use the final value theorem to find

$$\lim_{z \rightarrow 0} z \tilde{p}_0(z) = \lim_{z \rightarrow 0} \frac{1}{1 + \tilde{K}_{\text{avg}}(z)/z} \quad (30)$$

$$\lim_{t \rightarrow \infty} p_0(t) = \lim_{z \rightarrow 0} \left[1 + \int_0^\infty dt e^{-zt} \overbrace{\int_0^t d\tau K_{\text{avg}}(\tau)}^{\equiv \kappa(t)} \right]^{-1}.$$

If $\kappa(t)$ decays sufficiently quickly, we can extrapolate the $z \rightarrow 0$ limit from the finite times accessible from numerics. However, as we argued in the previous section, the memory cannot decay exponentially; therefore there is no single cutoff time t_c that can be used to approximate

$$\lim_{z \rightarrow 0} \int_0^\infty dt e^{-zt} \int_0^t d\tau K_{\text{avg}}(\tau) \approx \int_0^{t_c} dt \int_0^t d\tau K_{\text{avg}}(\tau).$$

The long time tail of $K_{\text{avg}}(t)$ has nonnegligible contributions to the dynamics, and therefore much care has to be taken in its use for extrapolations.

In lieu of a cutoff approximation, we turn again to the definition of K_{avg} ,

$$\tilde{K}_{\text{avg}}(z) = -z + \frac{1}{\tilde{p}_0(z)}. \quad (31)$$

The long time limit of the average population $\bar{p}_0(t)$ shall be denoted as p^∞ .

We take an ansatz for the memory at small z ,

$$\frac{\tilde{K}_{\text{avg}}(z)}{z} \approx p^\infty + a_0 z^{b_0} + a_1 z, \quad (32)$$

where $0 < b_0 < 1$. We note that the presence of terms like z^{b_0} is consistent with a power-law decay of $K_{\text{avg}}(t)$. Such an expansion for $\tilde{K}_{\text{avg}}(z)/z$ is motivated by the following argument on the analytic properties of $\tilde{p}_0(z)$. We first assume that the averaging procedure produces a continuum of poles on the imaginary axis with a smoothly varying distribution of residues $R(z)$ for $\tilde{p}_0(z)$,

$$\tilde{p}_0(z) = \frac{p^\infty}{z} + \int d\omega R(\omega) \frac{z}{z^2 + \omega^2}. \quad (33)$$

This leads to the formation of a branch cut on the imaginary axis. Therefore $\tilde{p}_0(z)$ cannot be expanded simply as a Laurent series about $z = 0$. Furthermore, $R(\omega)$ behaving as $\sim \omega^b$ introduces terms like z^{b+1} into the averaged population, in addition to the usual terms appearing in a Laurent expansion.

To extrapolate the long time populations, we compute $\kappa(t)$ defined in Eq. (30) and approximate its Laplace transform

$$\tilde{\kappa}(z) \approx \int_0^{t_{\text{max}}} dt e^{-zt} \kappa(t). \quad (34)$$

This result is then fitted using Eq. (32) to find p^∞ and b_0 and the amplitudes a_n . Such an approximation for the Laplace transform is admissible only if $\kappa(t)$ has decayed to sufficiently small values at $t = t_{\text{max}}$. We find that the results of using such an extrapolation procedure agree well with the values from independent calculations using exact diagonalization (Fig. 3). Thus we are able to obtain estimates for the long-time population of the central spin for system sizes ($L \gtrsim 16$) larger than those obtainable through exact diagonalization. In particular, this allows us to see how the central spin approaches the thermalized limit $p_0 = 1/2$ with increasing bath size. In the inset of Fig. 3, p_0 is consistent with power law decay $p_0 - 1/2 \sim L^{-0.8}$, which is roughly in line with the value given by the infinite temperature phase space average,

$$\frac{\mathcal{H}_{|0\rangle}(M^z = -1)}{\mathcal{H}(M^z = -1)} = \frac{\binom{L}{L/2}}{\binom{L+1}{L/2}} = \frac{1}{2} + \frac{1}{2(L+1)}, \quad (35)$$

measuring the relative sizes of the Hilbert spaces for eigenstates occupying $|0\rangle$ and $|1\rangle$. We stress that because the memory must decay with time, this procedure cannot be used in finite systems for a single disorder realization, as the population will generally not reach a steady state in such circumstances.

Finally, even though one can in principle apply the same ansatz to approximate $\tilde{p}_0(z)$ to directly extract p^∞ , this is likely not possible in practice. The difficulty lies in the fact that the signal for p^∞ in $\tilde{p}_0(z)$ comes through a z -dependence like $\tilde{p}_0(z) \sim p^\infty/z$. In order to obtain numerical data that faithfully reproduces this divergence, one must have already obtained $\bar{p}_0(t)$ to long times. If not, then one is constrained to attempt fitting $\tilde{p}_0(z)$ at relatively large value of z , where higher powers of z may

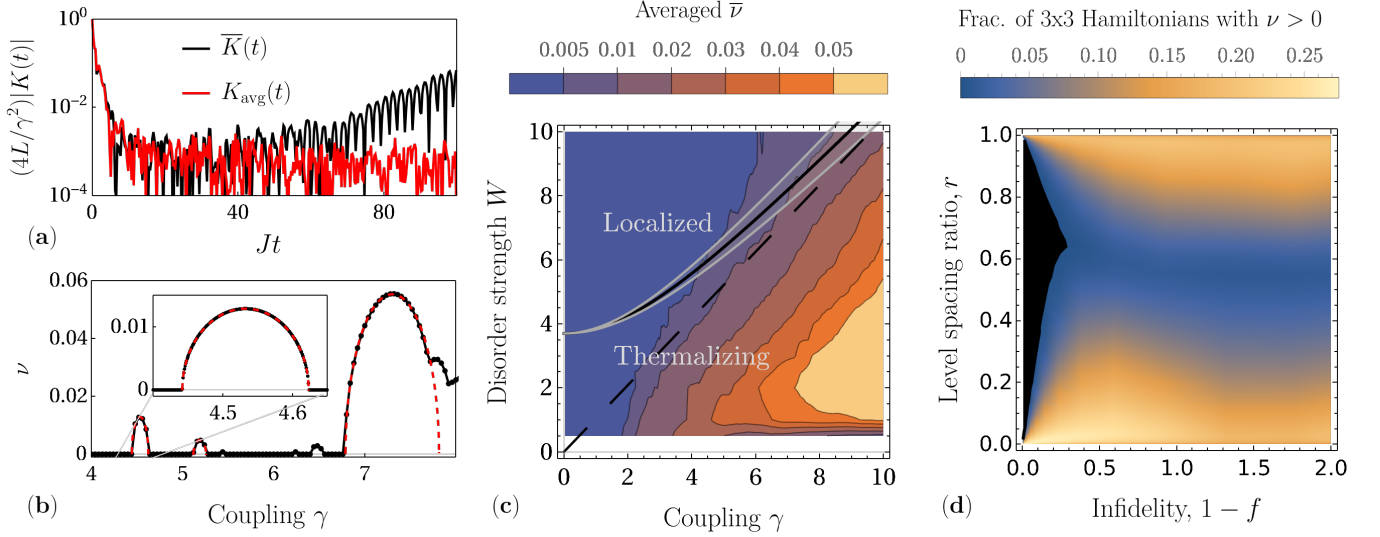


FIG. 4. (a) The averaged memory kernel \overline{K} and the memory kernel of the averaged dynamics K_{avg} , for $L = 14$ and $\gamma = 10$. The two curves are approximately the same up to $t \lesssim 40$, past which they diverge exponentially owing to certain disorder realizations contributing to \overline{K} . (b) Maximum rate ν of exponential growth for $L = 4$ across a range of couplings with a fixed realization of disorder. The rate is computed by solving for the poles of Laplace-transformed memory kernel using 4096 bits of precision. Transitions from zero ν to finite ν are sharply discontinuous, and are well captured by fits to half ellipses (dashed red lines). (c) Disorder averaged $\overline{\nu}$ for $L = 4$. The black line and its surrounding error bands indicate the $L \rightarrow \infty$ phase boundary determined in Ref. [31]. The dashed black line is the asymptotic behavior of the boundary as argued in Ref. [32]. (d) Fraction of random real 3×3 Hamiltonians which show nonzero ν . The fidelity $f \in [-1, 1]$ quantifies the minimum overlap between the eigenstates with the system-bath decoupled basis, with $f = 1$ when they coincide (see main text and appendix for details). Black regions indicate a fraction of exactly zero within the 10^7 random configurations of eigenvectors sampled. The level spacing ratio is defined as $r \equiv \min(E_2 - E_1, E_3 - E_2) / \max(E_2 - E_1, E_3 - E_2)$ where $E_1 < E_2 < E_3$.

be nonnegligible. The fact that the memory $K_{\text{avg}}(t)$ and its integral $\int_0^t d\tau K_{\text{avg}}(t)$ both decay to zero is what leads to the success of this method.

V. UNBOUNDED EXPONENTIAL GROWTH OF THE MEMORY KERNEL

We return now to the observation made in Sec. III C about memory kernels growing exponentially in time for certain realizations of the disorder. As seen in Fig. 4a, this can show up in the disorder averaged memory $\overline{K}(t)$, which can only be approximated via sampling over a finite number of disorder realizations. In Fig. 4b we show the maximum real part of the poles – corresponding to the maximum rate of exponential growth ν – for specific set of $\{h_i\}$ with $L = 4$. Intriguingly, ν is not monotonic with respect to γ , and displays square root singularities when going from $\nu = 0$ to finite ν . The sharpness of these singularities even with $L = 4$ indicates that they should not be associated with thermodynamic phase transitions. Instead, we believe they stem from exceptional points (EPs) in the generator of projected dynamics, $\mathbb{L}\mathbb{Q}$, which are related to generalized avoided crossings. This generator is responsible for the time evolution of the memory kernel, as seen in Eq. (7). By choosing to focus on only a subset of all the physical degrees of freedom in

the problem, we were forced to define projection operators \mathbb{P} that are not self-adjoint in the space of operators [64, 65]. For example, in operator space the projection operator associated with the scalar memory kernel is $\mathbb{P} = |0\rangle\langle 0| \otimes \hat{\rho}_B (|0\rangle\langle 0| \otimes \hat{I}_B)$, where the adjoint of the operator state vector has action

$$(\hat{A}|\hat{B}) = \text{Tr}(\hat{A}^\dagger \hat{B}). \quad (36)$$

The condition of being self-adjoint Liouville space is

$$\mathbb{P}^\dagger = \left(\sum_i |\hat{A}_i\rangle \langle \hat{B}_i| \right)^\dagger = \sum_i |\hat{B}_i\rangle \langle \hat{A}_i| = \mathbb{P}. \quad (37)$$

Writing \mathbb{P} in this way, it is clear that even if we project on to a thermal state of the bath, $\hat{\rho}_B \propto e^{-\beta H_B}$, the projector \mathbb{P} still cannot be self-adjoint unless the bath is in an infinite temperature state. Thus the projected Liouvillian $\mathbb{L}\mathbb{Q}$ is also not self-adjoint, a property which allows EPs to occur. We have additionally verified numerically that features unique to EPs such as the coalescence of eigenvalues and self-orthogonality are also present.

Interestingly, we note that the region in (W, γ) -space (Fig. 4c) for which MBL is predicted to be stable in the thermodynamic limit appears to be correlated with a suppressed ν . While we are currently unable to prove that this is not a coincidence – such system sizes cannot inform us about the stability of MBL – it is possible

that this provides a window into the character of the eigenstates, which are argued to be radically altered at large enough γ due to percolating networks of resonance states [32]. At the same time, it is known that the presence of exceptional points limits the radius of convergence for perturbative expansions [66, 67], and is postulated to be linked to quantum phase transitions [68, 69]. To fully explore any link between exceptional points, delocalization, and the breakdown of perturbative expansions will require a separate, in-depth study.

In the meantime, we can establish more indication of a connection between nonzero ν and localization in the following example in which an exponentially growing memory can occur. Consider a three-level system with non-degenerate eigenvalues $0 = E_1 < E_2 < E_3$. Since the overall scale of the energies does not matter, we can condense these into one parameter given by the level spacing ratio

$$r = \frac{\min(E_2 - E_1, E_3 - E_2)}{\max(E_2 - E_1, E_3 - E_2)}. \quad (38)$$

By fixing the energies we can sample random real Hamiltonians by generating random orthogonal matrices, whose columns constitute the eigenstates. To make connection with the reduced dynamics we consider in this paper, we generate these eigenstates in the system-bath decoupled basis, $|0\rangle \otimes |B_{1 \text{ or } 2}\rangle$ and $|1\rangle \otimes |B_3\rangle$. A linear combination of the basis states occupying $|0\rangle$ forms the initial state $\hat{\rho}(0)$. We quantify the relationship between the random eigenstates $|E_i\rangle$ and the decoupled basis $|SB_n\rangle$ through the fidelity,

$$F(E_1, E_2, E_3) = \min_{n=1,2,3} \max_{i=1,2,3} \langle E_i | SB_n \rangle, \quad (39)$$

and uniformly sample $|E_i\rangle$ to satisfy the constraint $f(E_1, E_2, E_3) \geq f$. The minimum fidelity f takes values between -1 and 1 . In Fig. 4d we show the maximum infidelity $1 - f$, which intuitively should play a similar role to the system bath coupling γ when both $1 - f$ and γ are small.

For each pair of (f, r) we can estimate the fraction of Hamiltonians and bath states – sampled uniformly subject to the constraint – that exhibit a nonzero ν . This result is shown in Fig. 4d. Exponential growth is seen to be prevalent near $r = 0$, which is when two eigenvalues of the Liouvillian become close to each other. This may be unsurprising given that exceptional points occur near level-crossings. More puzzling is the increasing prevalence of exponential growth as the level spacings become more uniform, i.e. as $r \rightarrow 1$. Finally, we observe zero instances of finite ν over 10^7 random samples of $|E_i\rangle$ inside a contiguous region beginning around $F \gtrsim 0.6$ (black region in Fig. 4d).

Heuristically speaking, delocalization with increasing coupling is the result of singular behavior in the full Hamiltonian, a fact which should be reflected in both the eigenstates and the spectrum. In finite systems, these may be isolated occurrences whose singular properties are

smoothed out upon taking expectation values. Our numerical observations suggest that the non-Hermiticity of the projected Liouvillian is highly sensitive to such singularities. We suspect this may be further indication of a deeper connection between localization and long-time pathologies in the memory kernel, but we are unable to clarify the underlying physics at this time.

VI. DISCUSSION AND OUTLOOK

In the model we have studied in this paper, we have taken the central coupling to scale to zero as γ/L , in accordance with Refs. [31, 32] which have argued for its necessity to perturbatively preserve localized eigenstates. As a consequence, we have argued that there arises a separation of timescales between the population dynamics (τ_{p_0}) and its associated memory kernel (τ_K). Should we repeat our arguments from Sec. III A with a central coupling scaling as γ/L^q , we find that these two timescales remain separated for $q > 1/2$, but coincide for $0 < q \leq 1/2$. It is not clear whether such a separation of timescales – where $\tau_{p_0} \gg \tau_K$ as $L \rightarrow \infty$ – is required for the preservation of localization. Heuristically speaking however, having $\tau_{p_0} \gg \tau_K$ does not appear at first glance to be strong enough to preserve all aspects of MBL. One of the dynamical hallmarks of MBL is a logarithmically slow spreading of entanglement, i.e. spins on sites i and $i + L/2$ become entangled after a timescale $\sim \exp(L/2\xi)$ with ξ being the localization length [36]. Based on our view of the system dynamics from the memory kernel, the interaction between these two sites mediated by the central qubit should proceed on a timescale growing as a power of L , which is much shorter than the dephasing time $\sim \exp(L/2\xi)$ and thus may accelerate the dephasing process responsible for the slow dynamics in the MBL phase. However, it was noted in Ref. [31] that the central qubit at best facilitates a subextensive transport of magnetization which augments, but does not destroy, the logarithmic growth of bipartite entanglement.

Our work also raises tantalizing questions about possible connections between poles of the Laplace-transformed memory kernel and thermalization/delocalization. To this end, some work [66, 70–72] has been done to connect the proliferation of exceptional points in non-Hermitian systems to the appearance of quantum phase transitions and chaos. By focusing on a subpart of a closed system, we are forced to consider non-Hermitian *Liouvillians* giving rise to exceptional points in the space of operators. Explorations in this direction may benefit from insights from the physics of Feshbach resonances. Of course, we are severely limited by the system sizes amenable to numerical studies, thus we are able to do little more than remark on the coincidences we observe.

On the more practical side, we have demonstrated that there may be enough information from finite time dynamics to yield knowledge about long time limits, should they exist. While we have only demonstrated the extrap-

olation to $t = \infty$ of the population of the central qubit, we should in principle be able to use the same memory kernel and the Nakajima-Zwanzig equation in Eq. (10) to extend the computed dynamics to longer times. That this is even possible should not be too surprising, given that Eq. (10) when discretized over time gives the same form as the ansatz underlying linear prediction [73, 74], a method widely used for extending dynamical calculations. What we have shown in this work is that there may be more physical content in such a procedure than was previously appreciated. To explore these ideas more thoroughly warrants careful attention, particularly in regard to stability and applicability, which we shall leave for future work.

Finally, we note that any possibility of a pathological memory kernel at real γ can be erased by choosing to work with self-adjoint projection superoperators \mathbb{P} . One may be interested in doing so, for example, in order to approximate system dynamics from low order, analytical expansions of the memory kernel. In that case it would

be beneficial to know that the error introduced by the approximation is not exponentially divergent with time. It is as yet unclear whether self-adjoint projectors necessarily yield improvements, since pathological behaviors can still occur for complex couplings γ to limit convergence of naïve series expansions. We note, however, that previous work [26, 75] saw benefits from applying symmetry-adapted “correlated projectors” – which, we should point out, are manifestly self-adjoint in Liouville space – to low order expansions of the memory kernel. We leave clarification of this point for future work.

Acknowledgements

We are grateful to Amikam Levy, Sebastian Wenderoth, and Michael Thoss for useful discussions. This research used resources of the National Energy Research Scientific Computing Center, a U.S. Department of Energy Office of Science User Facility operated under Contract No. DE-AC02-05CH11231.

-
- [1] J. Schliemann, A. Khaetskii, and D. Loss, *Journal of Physics: Condensed Matter* **15**, R1809 (2003).
 - [2] W. M. Witzel, M. S. Carroll, A. Morello, L. Cywiński, and S. Das Sarma, *Phys. Rev. Lett.* **105**, 187602 (2010).
 - [3] E. A. Chekhovich, M. N. Makhonin, A. I. Tartakovskii, A. Yacoby, H. Bluhm, K. C. Nowack, and L. M. K. Vandersypen, *Nature Materials* **12**, 494 (2013).
 - [4] D. Cogan, O. Kenneth, N. H. Lindner, G. Peniakov, C. Hopfmann, D. Dalacu, P. J. Poole, P. Hawrylak, and D. Gershoni, *Phys. Rev. X* **8**, 041050 (2018).
 - [5] R. Hanson, V. V. Dobrovitski, A. E. Feiguin, O. Gywat, and D. D. Awschalom, *Science* **320**, 352 (2008), <https://science.sciencemag.org/content/320/5874/352.full.pdf>.
 - [6] G. de Lange, T. van der Sar, M. Blok, Z.-H. Wang, V. Dobrovitski, and R. Hanson, *Scientific Reports* **2**, 382 (2012).
 - [7] E. Bauch, S. Singh, J. Lee, C. A. Hart, J. M. Schloss, M. J. Turner, J. F. Barry, L. M. Pham, N. Bar-Gill, S. F. Yelin, and R. L. Walsworth, *Phys. Rev. B* **102**, 134210 (2020).
 - [8] J. Dukelsky, S. Pittel, and G. Sierra, *Rev. Mod. Phys.* **76**, 643 (2004).
 - [9] P. W. Claeys, “Richardson-gaudin models and broken integrability,” (2018), [arXiv:1809.04447](https://arxiv.org/abs/1809.04447).
 - [10] T. Villazon, A. Chandran, and P. W. Claeys, *Phys. Rev. Research* **2**, 032052 (2020).
 - [11] M. Bortz and J. Stolze, *Phys. Rev. B* **76**, 014304 (2007).
 - [12] M. Bortz, S. Eggert, C. Schneider, R. Stübner, and J. Stolze, *Phys. Rev. B* **82**, 161308 (2010).
 - [13] E. Barnes, L. Cywiński, and S. Das Sarma, *Phys. Rev. Lett.* **109**, 140403 (2012).
 - [14] L. T. Hall, J. H. Cole, and L. C. L. Hollenberg, *Phys. Rev. B* **90**, 075201 (2014).
 - [15] F. A. Wolf, I. P. McCulloch, and U. Schollwöck, *Phys. Rev. B* **90**, 235131 (2014).
 - [16] H. Wang and J. Shao, *The Journal of Chemical Physics* **137**, 22A504 (2012), <https://doi.org/10.1063/1.4732808>.
 - [17] L. Diósi and W. T. Strunz, *Physics Letters A* **235**, 569 (1997).
 - [18] P. P. Orth, A. Imambekov, and K. Le Hur, *Phys. Rev. B* **87**, 014305 (2013).
 - [19] L. P. Lindoy and D. E. Manolopoulos, *Phys. Rev. Lett.* **120**, 220604 (2018).
 - [20] A. Faribault and D. Schuricht, *Phys. Rev. B* **88**, 085323 (2013).
 - [21] A. J. Leggett, S. Chakravarty, A. T. Dorsey, M. P. A. Fisher, A. Garg, and W. Zwerger, *Rev. Mod. Phys.* **59**, 1 (1987).
 - [22] N. V. Prokof'ev and P. C. E. Stamp, *Reports on Progress in Physics* **63**, 669 (2000).
 - [23] A. Khaetskii, D. Loss, and L. Glazman, *Phys. Rev. B* **67**, 195329 (2003).
 - [24] W. A. Coish and D. Loss, *Phys. Rev. B* **70**, 195340 (2004).
 - [25] G. Chen, D. L. Bergman, and L. Balents, *Phys. Rev. B* **76**, 045312 (2007).
 - [26] E. Barnes, L. Cywiński, and S. Das Sarma, *Phys. Rev. B* **84**, 155315 (2011).
 - [27] B. Erbe and J. Schliemann, *Phys. Rev. B* **85**, 235423 (2012).
 - [28] X. Zhou, Q.-K. Wan, and X.-H. Wang, *Entropy* **22** (2020).
 - [29] R. I. Nepomechie and X.-W. Guan, *Journal of Statistical Mechanics: Theory and Experiment* **2018**, 103104 (2018).
 - [30] J. Jing and L.-A. Wu, *Scientific Reports* **8**, 1471 (2018).
 - [31] D. Hetterich, N. Y. Yao, M. Serbyn, F. Pollmann, and B. Trauzettel, *Phys. Rev. B* **98**, 161122 (2018).
 - [32] P. Ponte, C. R. Laumann, D. A. Huse, and A. Chandran, *Phil. Trans. R. Soc. A* **375** (2017), 10.1098/rsta.2016.0428.
 - [33] D. A. Huse, R. Nandkishore, and V. Oganesyan, *Phys. Rev. B* **90**, 174202 (2014).
 - [34] R. Nandkishore and D. A. Huse, *Annual Re-*

- view of Condensed Matter Physics **6**, 15 (2015), <https://doi.org/10.1146/annurev-conmatphys-031214-014726>.
- [35] J. Z. Imbrie, V. Ros, and A. Scardicchio, *Annalen der Physik* **529**, 1600278 (2017), <https://onlinelibrary.wiley.com/doi/pdf/10.1002/andp.201600278> (2015), arXiv:1509.04352 [quant-ph].
- [36] D. A. Abanin, E. Altman, I. Bloch, and M. Serbyn, *Rev. Mod. Phys.* **91**, 021001 (2019).
- [37] M. Žnidarič, T. c. v. Prosen, and P. Prelovšek, *Phys. Rev. B* **77**, 064426 (2008).
- [38] J. H. Bardarson, F. Pollmann, and J. E. Moore, *Phys. Rev. Lett.* **109**, 017202 (2012).
- [39] Y. Bar Lev, G. Cohen, and D. R. Reichman, *Phys. Rev. Lett.* **114**, 100601 (2015).
- [40] G. De Tomasi, F. Pollmann, and M. Heyl, *Phys. Rev. B* **99**, 241114 (2019).
- [41] F. Alet and N. Laflorencie, *Comptes Rendus Physique* **19**, 498 (2018), quantum simulation / Simulation quantique.
- [42] T. Chanda, P. Sierant, and J. Zakrzewski, *Phys. Rev. Research* **2**, 032045 (2020).
- [43] G. Cohen and E. Rabani, *Phys. Rev. B* **84**, 075150 (2011).
- [44] G. Cohen, E. Gull, D. R. Reichman, A. J. Millis, and E. Rabani, *Phys. Rev. B* **87**, 195108 (2013).
- [45] E. Y. Wilner, H. Wang, M. Thoss, and E. Rabani, *Phys. Rev. B* **89**, 205129 (2014).
- [46] E. Y. Wilner, H. Wang, G. Cohen, M. Thoss, and E. Rabani, *Phys. Rev. B* **88**, 045137 (2013).
- [47] R. Zwanzig, “Statistical mechanics of irreversibility,” in *Lectures in Theoretical Physics*, Vol. 3, edited by W. E. Brittin, B. W. Downs, and J. Downs (New York, 1961) p. 106–141.
- [48] H.-P. Breuer, F. Petruccione, *et al.*, *The theory of open quantum systems* (Oxford University Press, 2002).
- [49] N. Singh, *Electronic Transport Theories* (CRC Press, 2016).
- [50] L. Kidon, H. Wang, M. Thoss, and E. Rabani, *The Journal of Chemical Physics* **149**, 104105 (2018), <https://doi.org/10.1063/1.5047446>.
- [51] G. Ithier and F. Benaych-Georges, *Phys. Rev. A* **96**, 012108 (2017).
- [52] Note that this does *not* make any statement about the existence of a limiting curve as the size of the bath $L \rightarrow \infty$. This result only quantifies the magnitude of the fluctuations in the system’s dynamics for a given, fixed bath size.
- [53] While this type of transformation generally hides global topological properties, it should preserve local dynamics, particularly that of the central qubit’s, which is what we are solely interested in.
- [54] R. Kosloff, *Annual Review of Physical Chemistry* **45**, 145 (1994), <https://doi.org/10.1146/annurev.pc.45.100194.001045>.
- [55] A. Weiße, G. Wellein, A. Alvermann, and H. Fehske, *Rev. Mod. Phys.* **78**, 275 (2006).
- [56] S. Gopalakrishnan, M. Müller, V. Khemani, M. Knap, E. Demler, and D. A. Huse, *Phys. Rev. B* **92**, 104202 (2015).
- [57] S. Gopalakrishnan and S. Parameswaran, *Physics Reports* **862**, 1 (2020), dynamics and transport at the threshold of many-body localization.
- [58] A. Nitzan, *Chemical Dynamics in Condensed Phases* (Oxford University Press, 2006).
- [59] L. Rademaker and M. Ortuño, *Phys. Rev. Lett.* **116**, 010404 (2016).
- [60] D. Pekker, B. K. Clark, V. Oganessian, and G. Refael, *Phys. Rev. Lett.* **119**, 075701 (2017).
- [61] L. Campos Venuti, arXiv e-prints, arXiv:1509.04352 (2015), arXiv:1509.04352 [quant-ph].
- [62] C. M. Kropf, C. Gneiting, and A. Buchleitner, *Phys. Rev. X* **6**, 031023 (2016).
- [63] Note that this argument does not exclude the possibility of oscillations resulting from analogs of limit cycles in classical dynamics, nor does it exclude fast timescales due to a finite disorder-averaged bandwidth.
- [64] J. Wilkie, *The Journal of Chemical Physics* **114**, 7736 (2001).
- [65] J. Wilkie, *The Journal of Chemical Physics* **115**, 10335 (2001).
- [66] W. D. Heiss, *Journal of Physics A: Mathematical and Theoretical* **45**, 444016 (2012).
- [67] A. Marie, H. G. A. Burton, and P.-F. Loos, *Journal of Physics: Condensed Matter* (2021).
- [68] C. Jung, M. Müller, and I. Rotter, *Phys. Rev. E* **60**, 114 (1999).
- [69] S. Garmon, I. Rotter, N. Hatano, and D. Segal, *International Journal of Theoretical Physics* **51**, 3536 (2012).
- [70] W. D. Heiss and A. L. Sannino, *Journal of Physics A: Mathematical and General* **23**, 1167 (1990).
- [71] P. Stránský, M. Dvořák, and P. Cejnar, *Phys. Rev. E* **97**, 012112 (2018).
- [72] P. Cejnar, S. Heinze, and M. Macek, *Phys. Rev. Lett.* **99**, 100601 (2007).
- [73] T. Barthel, U. Schollwöck, and S. R. White, *Phys. Rev. B* **79**, 245101 (2009).
- [74] U. Schollwöck, *Annals of Physics* **326**, 96 (2011), january 2011 Special Issue.
- [75] J. Fischer and H.-P. Breuer, *Phys. Rev. A* **76**, 052119 (2007).

Supplemental Material for “Signatures of a localizable bath in the memory kernel of a generalized quantum master equation”

Appendix A: Numerical inversion for memory

Here we summarize the numerical methods used to investigate the memory kernel. For simplicity we shall restrict ourselves to the case of $H_S = 0$ with matrix memory kernels \mathbb{K} and system propagators \mathbb{U}_S :

$$\frac{d}{dt}\mathbb{U}_S(t) = - \int_0^t dt' \mathbb{K}(t')\mathbb{U}_S(t-t').$$

We assume that the value of $\mathbb{K}(0)$ is known, a fact which allows us to use slightly higher order approximations. For a general bath state ρ_B , the initial value is $\gamma_{\perp}^2 \sum_{i,j,\pm} \text{Tr} [\hat{\sigma}_i^{\pm} \hat{\sigma}_j^{\mp} \rho_B]$.

We discretize this equation as follows:

$$\begin{aligned} \dot{\mathbb{U}}_S(n\Delta t) &= \frac{1}{\Delta t} \left(\frac{-\mathbb{U}_S((n-1)\Delta t)}{3} + \frac{-\mathbb{U}_S(n\Delta t)}{2} + \mathbb{U}_S((n+1)\Delta t) + \frac{-\mathbb{U}_S((n+2)\Delta t)}{6} \right) + O(\Delta t^3) \\ \int_0^{n\Delta t} dt' \mathbb{K}(t')\mathbb{U}_S(n\Delta t - t') &= (\Delta t) \left(\frac{\mathbb{K}(0\Delta t)\mathbb{U}_S(n\Delta t) + \mathbb{K}(n\Delta t)\mathbb{U}_S(0\Delta t)}{2} + \sum_{m=1}^{n-1} \mathbb{K}(m\Delta t)\mathbb{U}_S((n-m)\Delta t) \right) + O(\Delta t^3). \end{aligned}$$

The calculations in the main paper were performed with $J\Delta t = 0.01$ for $0 \leq Jt \leq 100$. By truncating the error terms and equating the two expressions, the memory kernel can be solved for via iterating back substitutions. We note that the numerically inverted solution displays spurious oscillations of period $2\Delta t$. This can be largely removed by taking the 2-element moving average, i.e.

$$\mathbb{K}\left((n + \frac{1}{2})\Delta t\right) = \frac{\mathbb{K}(n\Delta t) + \mathbb{K}((n+1)\Delta t)}{2}.$$

For example, in the case of a scalar memory kernel generating the dynamics such that $K(t) = \exp(-t/5) \cos(t)$, such an averaging procedure produces a much more well-behaved solution (see Figure 5).

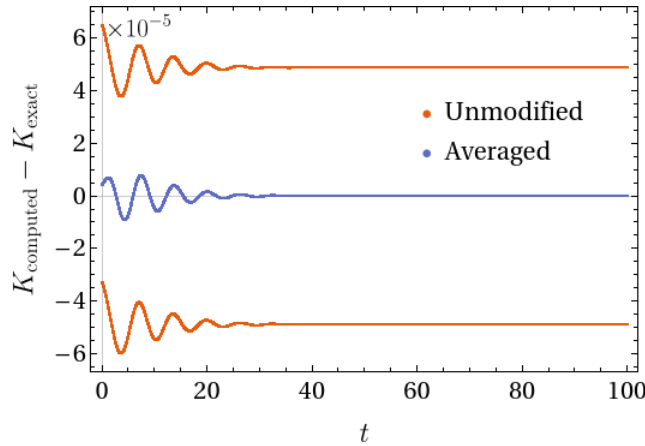


FIG. 5. Numerical inversion of dynamics generated by the memory kernel $K(t) = \exp(-t/5) \cos(t)$, compared against the exact solution. Without the 2-element moving average, the computed memory oscillates between the top and bottom bands on each timestep $\Delta t = 0.01$.

Appendix B: Scalar memory kernel

The memory kernel superoperator can be reduced to one function if we specify that we are interested only in the $|0\rangle\langle 0|$ population of the reduced density matrix for the system. The relevant projection superoperator is

$$\mathbb{P}\rho = (|0\rangle\langle 0| \otimes \rho_B) \text{Tr} \left((|0\rangle\langle 0| \otimes \hat{I}_B) \rho \right),$$

and the memory kernel (now a scalar function) is follows the same form as before:

$$K(t) = \text{Tr} [\text{PLQ} e^{-i\text{QLQ}t} \text{QLP}]. \quad (\text{B1})$$

The scalar memory kernel can be related to the two independent entries $\mathbb{K}_{(00),(00)}$ and $\mathbb{K}_{(11),(11)}$ of the matrix-valued memory kernel via a series of convolutions,

$$\begin{aligned} K(t) &= \int_0^t d\tau \mathbb{K}_{(00),(00)}(t-\tau) \dot{G}_1(\tau) \\ \dot{G}_1(t) &= - \int_0^t d\tau \mathbb{K}_{(11),(11)}(t-\tau) G_1(\tau). \end{aligned}$$

This gives a master equation

$$\dot{p}_0(t) = - \int_0^t d\tau K(t-\tau) p_0(\tau).$$

Note, however, that the equivalent expression derived from the matrix-valued memory kernel is

$$\dot{\sigma}_{(00),(00)}(t) \equiv \dot{p}_0(t) = \int_0^t d\tau \mathbb{K}_{(11),(11)}(\tau) - \int_0^t d\tau (\mathbb{K}_{(00),(00)}(t-\tau) + \mathbb{K}_{(11),(11)}(t-\tau)) p_0(\tau).$$

The difference between these two expressions is that, in the former case where the scalar memory kernel is directly defined from a suitable projection operator, the state $|1\rangle$ in the central qubit is explicitly treated as part of the bath. In the second case where this was not done, the influence of the $|1\rangle$ state on the population of the $|0\rangle$ state manifests as an external fluctuating force, $\int_0^t \mathbb{K}_{(11),(11)}(\tau) d\tau$.

We can quickly derive the memory kernel in the eigenbasis by virtue of its relation with the trajectory $p_0(t)$. In the following, we adopt the notation: $|\psi_0\rangle$ denotes the initial bath state; $|0, B\rangle$ denotes the factorized state where the system is in $|0\rangle$ and the bath is in $|B\rangle$; and $|E\rangle$ denotes the eigenstate of energy E of the combined system and bath. The population, in the time and Laplace domains, is given by

$$\begin{aligned} p_0(t) &= \sum_B \left| \sum_E e^{-iEt} \langle 0, B|E\rangle \langle E|0, \psi_0\rangle \right|^2 \\ &= \sum_B \sum_{E, E'} e^{-i(E-E')t} \langle 0, \psi_0|E'\rangle \langle E'|0, B\rangle \langle 0, B|E\rangle \langle E|0, \psi_0\rangle \\ p_0(z) &= \sum_{E, E'} \underbrace{\left(\sum_B \langle E'|0, B\rangle \langle 0, B|E\rangle \right)}_{\equiv C(E', E)} \frac{\langle 0, \psi_0|E'\rangle \langle E|0, \psi_0\rangle}{z + i(E - E')}. \end{aligned}$$

Since the memory kernel is defined in as $K(z) = -z + p_0(z)^{-1}$, we therefore have, after using the fact that the inner products in the above expression are real,

$$K(z) = -z + \left(\sum_E \frac{C(E, E) |\langle E|0, \psi_0\rangle|^2}{z} + 2z \sum_{E' > E} C(E', E) \frac{\langle 0, \psi_0|E'\rangle \langle E|0, \psi_0\rangle}{z^2 + (E - E')^2} \right)^{-1}$$

Appendix C: Appearance of complex poles for the scalar memory kernel

To verify the exponential growth of $K(t)$ we observe from directly inverting the Nakajima-Zwanzig equation in the time domain, we solve for the poles of $\tilde{K}(z)$ numerically using 4096 bits of precision. Diagonalization and root-finding are respectively provided by the `GenericLinearAlgebra.jl` and the `PolynomialRoots.jl` packages in Julia. The rapid growth of the Liouville space's dimensionality limits this approach to system sizes $L \leq 6$.

The scalar memory kernel in Laplace space has a very simple form,

$$K(z) = -z + \left(\frac{\overline{p_0}}{z} + \sum_{n=1}^N \frac{A_n z}{z^2 + \omega_n^2} \right)^{-1},$$

where $\bar{p}_0 > 0$ is the value that $p_0(t)$ either decays to or oscillates around as $t \rightarrow \infty$. The frequencies ω_n are given by the difference of the n th pair of energies of the full Hamiltonian, $\omega_n = E' - E$ such that $E' > E$. The initial value of $p_0(0) = 1$ sets a constraint that $\bar{p}_0 + \sum_n A_n = 1$. The requirement that $0 \leq p_0 \leq 1$ gives the pair of sufficient conditions $\bar{p}_0 + \sum_n |A_n| \leq 1$ and $0 \leq \bar{p}_0 - \sum_n |A_n|$.

1. Three eigenvalues

The system of three states is simplest one for analyzing the exponential growth in the scalar memory kernel, since it yields only three unique positive energy differences. This in turn leads to a cubic equation $f_3(x)$ for the poles of the memory kernel, and the roots of cubic equations are well characterized by the sign of the discriminant. WLOG, we define $\omega_1 = \Omega$, $\omega_2 = \delta$, and $\omega_3 = \Omega + \delta$, and the ratio of adjacent energy differences $r \equiv \delta/\Omega$. Since the physics should be invariant with respect to swapping Ω and δ , we shall limit our discussion of r on the restricted domain $[0, 1]$.

$$\begin{aligned} f_3(z^2) &= (z^2)^3 + \underbrace{((1 - A_1)\omega_1^2 + (1 - A_2)\omega_2^2 + (1 - A_3)\omega_3^2)}_{\equiv b} (z^2)^2 \\ &\quad + \underbrace{((\bar{p}_0 + A_1)\omega_2^2\omega_3^2 + (\bar{p}_0 + A_2)\omega_1^2\omega_3^2 + (\bar{p}_0 + A_3)\omega_1^2\omega_2^2)}_{\equiv c} (z^2)^1 \\ &\quad + \underbrace{\bar{p}_0\omega_1^2\omega_2^2\omega_3^2}_{\equiv d} \end{aligned}$$

This is a real cubic polynomial in the variable $x \equiv z^2$. The properties of its zeroes are communicated through the sign of its discriminant Δ , which for a general cubic equation $ax^3 + bx^2 + cx + d$ is given by

$$\Delta = b^2c^2 - 4ac^3 - 4b^3d - 27a^2d^2 + 18abcd.$$

When this quantity is negative, the equation will have two complex roots. Similarly, if $\Delta > 0$ and the coefficients of f_3 are strictly positive, there must be three real, negative roots. Assuming that $\bar{p}_0 > 0$ implies $d > 0$. We can therefore work with a modified discriminant by dividing through by d^2 , while retaining the properties of the original discriminant. Doing so results in

$$\begin{aligned} \Delta' &= \beta^2\gamma^2 + 18\beta\gamma - 4\gamma^3 - 4\beta^3 - 27 \\ \beta &= b/d^{1/3} \\ \gamma &= \gamma/d^{2/3} \end{aligned}$$

In terms of the ratio r , we have

$$\begin{aligned} \beta &= \frac{1}{\bar{p}_0^{1/3}} \left((1 - A_1)r^{-2/3}(1 + r)^{-2/3} + (1 - A_2)r^{4/3}(1 + r)^{-2/3} + (1 - A_3)r^{-2/3}(1 + r)^{4/3} \right) \\ \gamma &= \frac{1}{\bar{p}_0^{2/3}} \left((\bar{p}_0 + A_1)r^{2/3}(1 + r)^{2/3} + (\bar{p}_0 + A_2)r^{-4/3}(1 + r)^{2/3} + (\bar{p}_0 + A_3)r^{2/3}(1 + r)^{-4/3} \right) \end{aligned}$$

We find that the sufficient conditions provided by the bounds $0 \leq p_0 \leq 1 \implies \bar{p}_0 + \sum_n |A_n| \leq 1$ and $0 \leq \bar{p}_0 - \sum_n |A_n|$ is too strict and evidently produces no complex poles. Instead, we shall randomly sample the A_n 's and \bar{p}_0 .

In this three-state case, we parametrize the eigenstates using the axis-angle representation, where for the k th eigenstate ($k = 1, 2, 3$),

$$\left(\mathbf{v}^{(k)} \right)_j = \left(e^{-i\theta(\hat{\mathbf{S}} \cdot \mathbf{n})} \right)_{j,k},$$

where the unit vector \mathbf{n} is defined by the polar angle ψ and the azimuthal angle ϕ . In terms of these three parameters, we define probability distribution as

$$P(\phi, \psi, \theta) d\phi d\psi d\theta = \frac{\sin \psi}{4\pi} \frac{1 - \cos \theta}{\theta_{\max} - \sin \theta_{\max}} d\phi d\psi d\theta,$$

on the domain $0 \leq \phi < 2\pi$, $0 \leq \psi \leq \pi$, and $0 \leq \theta \leq \theta_{\max}$, where $0 \leq \theta_{\max} \leq \pi$. As seen in Fig. 6, the angle θ_{\max} measures the maximum deviation between the eigenvectors and the system=bath decoupled basis states. This measure coincides with the Haar measure for the 3×3 circular orthogonal ensemble When $\theta_{\max} = \pi$. In the main text, we measure this deviation in terms of the minimum fidelity

$$f \equiv \cos \theta_{\max}.$$

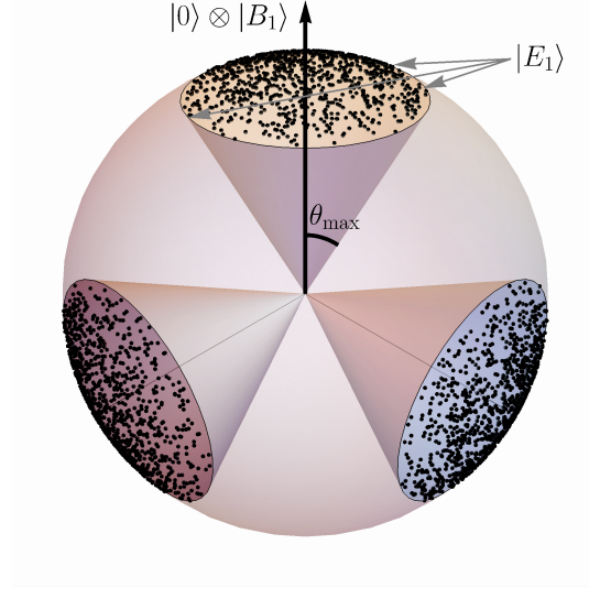


FIG. 6. Relationship between the system-bath decoupled basis (unit vectors on the x, y, z axes) and the randomly sampled eigenvectors (black dots). The parameter θ_{\max} controls the maximum deviation of the eigenvectors from the basis (shaded regions bounded by cones).

Appendix D: Short time behavior of the memory kernel

In this section we reproduce the calculation for the short time behavior of the scalar memory kernel $K(t)$. The zeroth and second derivatives of $K(t)$ at $t = 0$ are given respectively by

$$K(t=0) = -p_0^{(2)}(t=0) \quad (\text{D1})$$

$$K^{(2)}(t=0) = -p_0^{(4)}(t=0) + \left(p_0^{(2)}(t=0)\right)^2. \quad (\text{D2})$$

For a single realization of disorder, we therefore need

$$\begin{aligned} p_0^{(2)}(t=0) &= -\text{Tr} \left((|0\rangle\langle 0| \otimes \hat{I}_B) [H, [H, |0\rangle\langle 0| \otimes \rho_B]] \right) \\ p_0^{(4)}(t=0) &= \text{Tr} \left((|0\rangle\langle 0| \otimes \hat{I}_B) [H, [H, [H, [H, |0\rangle\langle 0| \otimes \rho_B]]]] \right). \end{aligned}$$

Throughout the calculation we shall rely on the Pauli algebra,

$$[\hat{\sigma}^z, \hat{\sigma}^\pm] = \pm 2\hat{\sigma}^\pm \quad [\hat{\sigma}^+, \hat{\sigma}^-] = \hat{\sigma}^z \quad \{\hat{\sigma}^z, \hat{\sigma}^\pm\} = 0 \quad \{\hat{\sigma}^+, \hat{\sigma}^-\} = \hat{I},$$

along with the commutator identity for operators A_i that commute with B_i but not within each group,

$$[A_1 B_1, A_2 B_2] = [A_1, A_2] B_1 B_2 + A_2 A_1 [B_1, B_2] \quad (\text{D3})$$

$$= [A_1, A_2] \frac{\{B_1, B_2\}}{2} + \frac{\{A_2, A_1\}}{2} [B_1, B_2]. \quad (\text{D4})$$

We shall also make use of the following identity to reduce the number of nested commutators:

$$\text{Tr} (A [B, C]) = -\text{Tr} ([B, A] C).$$

In the following we shall assume that $[\sum_i \hat{\sigma}_i^z, \rho_B] = [\sum_i \hat{\sigma}_i^z, H_B] = 0$. The first commutators can be reduced to

$$\begin{aligned}
[H, |0\rangle\langle 0| \otimes \hat{I}_B] &= \cancel{[H_S, |0\rangle\langle 0| \otimes \hat{I}_B]}^0 + \cancel{[H_B, |0\rangle\langle 0| \otimes \hat{I}_B]}^0 + [V, |0\rangle\langle 0| \otimes \hat{I}_B] \\
&= \gamma_\perp \sum_{i=1}^L \sum_{\pm} [\hat{\tau}^\pm \hat{\sigma}_i^\mp, |0\rangle\langle 0| \otimes \hat{I}_B] + \gamma_z \sum_{i=1}^L [\hat{\tau}^z \hat{\sigma}_i^z, |0\rangle\langle 0| \otimes \hat{I}_B] \\
&= \gamma_\perp \sum_{i=1}^L |1\rangle\langle 0| \otimes \hat{\sigma}_i^- - |0\rangle\langle 1| \otimes \hat{\sigma}_i^+ \\
[H, |0\rangle\langle 0| \otimes \hat{\rho}_B] &= \cancel{[H_S, |0\rangle\langle 0| \otimes \hat{\rho}_B]}^0 + [H_B, |0\rangle\langle 0| \otimes \hat{\rho}_B] + [V, |0\rangle\langle 0| \otimes \hat{\rho}_B] \\
&= |0\rangle\langle 0| \otimes [H_B, \hat{\rho}_B] + \gamma_\perp \sum_{i=1}^L \sum_{\pm} [\hat{\tau}^\pm \hat{\sigma}_i^\mp, |0\rangle\langle 0| \otimes \hat{\rho}_B] + \gamma_z \left[\hat{\tau}^z \otimes \left(\sum_{i=1}^L \hat{\sigma}_i^z \right), |0\rangle\langle 0| \otimes \hat{\rho}_B \right] \\
&= |0\rangle\langle 0| \otimes [H_B, \hat{\rho}_B] + \gamma_\perp \sum_{i=1}^L |1\rangle\langle 0| \otimes (\hat{\sigma}_i^- \hat{\rho}_B) - |0\rangle\langle 1| \otimes (\hat{\rho}_B \hat{\sigma}_i^+).
\end{aligned}$$

These two expressions allow us to immediately evaluate $p_0^{(2)}(t=0)$, giving

$$\begin{aligned}
-p_0^{(2)}(t=0) &= \gamma_\perp \text{Tr} \left\{ \left(\sum_{j=1}^L |0\rangle\langle 1| \otimes \hat{\sigma}_j^+ - |1\rangle\langle 0| \otimes \hat{\sigma}_j^- \right) \left(|0\rangle\langle 0| \otimes [H_B, \hat{\rho}_B] + \gamma_\perp \sum_{i=1}^L |1\rangle\langle 0| \otimes (\hat{\sigma}_i^- \hat{\rho}_B) - |0\rangle\langle 1| \otimes (\hat{\rho}_B \hat{\sigma}_i^+) \right) \right\} \\
&= \gamma_\perp^2 \sum_{i,j=1}^L \text{Tr} \{ (|0\rangle\langle 1| \otimes \hat{\sigma}_j^+ - |1\rangle\langle 0| \otimes \hat{\sigma}_j^-) (|1\rangle\langle 0| \otimes (\hat{\sigma}_i^- \hat{\rho}_B) - |0\rangle\langle 1| \otimes (\hat{\rho}_B \hat{\sigma}_i^+)) \} \\
&= \gamma_\perp^2 \sum_{i,j=1}^L \text{Tr} (|0\rangle\langle 0| \otimes (\hat{\sigma}_j^+ \hat{\sigma}_i^- \hat{\rho}_B) + |1\rangle\langle 1| \otimes (\hat{\rho}_B \hat{\sigma}_i^+ \hat{\sigma}_j^-)) \\
&= \gamma_\perp^2 \sum_{i,j=1}^L \text{Tr}_B (\{\hat{\sigma}_j^+, \hat{\sigma}_i^-\} \hat{\rho}_B) = \gamma_\perp^2 \sum_{i,j=1}^L \text{Tr}_B (\{\hat{\sigma}_j^+, \hat{\sigma}_i^-\} \hat{\rho}_B) \\
&= L\gamma_\perp^2 + \gamma_\perp^2 \sum_{i \neq j}^L \text{Tr}_B (\{\hat{\sigma}_j^+, \hat{\sigma}_i^-\} \hat{\rho}_B).
\end{aligned}$$

When the initial bath state has a single pattern of magnetization (i.e. it is a product state of $\hat{\sigma}_i^z$ eigenstates), the initial value of the memory kernel will be $K(t=0) = L\gamma_\perp^2$, independent of the disorder realization as well as intrabath interactions. The fact that $K^{(2)}(t=0)$ is linear in the disorder-dependent quantity $p_0^{(4)}(t=0)$, when combined with the disorder-independence of $p_0^{(2)}(t=0)$, implies at least at short times it does not matter when the disorder averaging is performed. That is, averaging p_0 before calculating $K(t)$ will give the same result as averaging over all $K(t)$ associated with each realization of p_0 . This gives an explicit example of our claim that for short times $K_{\text{avg}}(t) \approx \bar{K}(t)$.

Evaluation of the fourth derivative for p_0 is more involved, but proceeds along a similar route. Generally speaking, note that these derivatives rely on the dynamics of coherences (i.e. off-diagonal elements) in the full density matrix.

$$\begin{aligned}
[H, [H, |0\rangle\langle 0| \otimes \hat{I}_B]] &= \gamma_\perp [H, \hat{\tau}^+ \otimes \hat{M}_B^- - \hat{\tau}^- \otimes \hat{M}_B^+] \\
&= \gamma_\perp \left(\hat{\tau}^+ \otimes [H_B, \hat{M}_B^-] - \hat{\tau}^- \otimes [H_B, \hat{M}_B^+] \right) \\
&\quad + \gamma_\perp \gamma_z \left(\hat{\tau}^+ \otimes \{\hat{M}_B^z, \hat{M}_B^-\} + \hat{\tau}^- \otimes \{\hat{M}_B^z, \hat{M}_B^+\} \right) \\
&\quad + \gamma_\perp^2 \left(|0\rangle\langle 0| \otimes (\hat{M}_B^+ \hat{M}_B^- + \hat{M}_B^- \hat{M}_B^+) - |1\rangle\langle 1| \otimes (\hat{M}_B^- \hat{M}_B^+ + \hat{M}_B^+ \hat{M}_B^-) \right)
\end{aligned}$$

$$\begin{aligned}
[H, [H, |0\rangle\langle 0| \otimes \hat{\rho}_B]] &= \left[H, |0\rangle\langle 0| \otimes [H_B, \hat{\rho}_B] + \gamma_\perp \left(\hat{\tau}^+ \otimes \hat{M}_B^- \hat{\rho}_B - \hat{\tau}^- \otimes \hat{\rho}_B \hat{M}_B^+ \right) \right] \\
&= |0\rangle\langle 0| \otimes [H_B, [H_B, \hat{\rho}_B]] \\
&\quad + \gamma_\perp \left(\hat{\tau}^+ \otimes [H_B, \hat{M}_B^- \hat{\rho}_B] - \hat{\tau}^- \otimes [H_B, \hat{\rho}_B \hat{M}_B^+] \right) \\
&\quad + \gamma_\perp \left(\hat{\tau}^+ \otimes \hat{M}_B^- [H_B, \hat{\rho}_B] - \hat{\tau}^- \otimes [H_B, \hat{\rho}_B] \hat{M}_B^+ \right) \\
&\quad + \gamma_\perp \gamma_z \left(\hat{\tau}^z |0\rangle\langle 0| \otimes \left[\hat{M}_B^z, [H_B, \hat{\rho}_B] \right] + \hat{\tau}^+ \otimes \left\{ \hat{M}_B^z, \hat{M}_B^- \hat{\rho}_B \right\} + \hat{\tau}^- \otimes \left\{ \hat{M}_B^z, \hat{\rho}_B \hat{M}_B^+ \right\} \right) \\
&\quad + \gamma_\perp^2 \left(|0\rangle\langle 0| \otimes \left(\hat{M}_B^+ \hat{M}_B^- \hat{\rho}_B + \hat{\rho}_B \hat{M}_B^+ \hat{M}_B^- \right) - |1\rangle\langle 1| \otimes \left(\hat{M}_B^- \hat{\rho}_B \hat{M}_B^+ + \hat{M}_B^- \hat{\rho}_B \hat{M}_B^+ \right) \right) \\
&= |0\rangle\langle 0| \otimes [H_B, [H_B, \hat{\rho}_B]] \\
&\quad + \gamma_\perp \left(\hat{\tau}^+ \otimes [H_B, \hat{M}_B^- \hat{\rho}_B] - \hat{\tau}^- \otimes [H_B, \hat{\rho}_B \hat{M}_B^+] \right) \\
&\quad + \gamma_\perp \left(\hat{\tau}^+ \otimes \hat{M}_B^- [H_B, \hat{\rho}_B] - \hat{\tau}^- \otimes [H_B, \hat{\rho}_B] \hat{M}_B^+ \right) \\
&\quad - 2\gamma_\perp \gamma_z \left(\hat{\tau}^+ \otimes \hat{M}_B^- \hat{\rho}_B + \hat{\tau}^- \otimes \hat{\rho}_B \hat{M}_B^+ \right) \\
&\quad + \gamma_\perp^2 \left(|0\rangle\langle 0| \otimes \left(\hat{M}_B^+ \hat{M}_B^- \hat{\rho}_B + \hat{\rho}_B \hat{M}_B^+ \hat{M}_B^- \right) - |1\rangle\langle 1| \otimes \left(\hat{M}_B^- \hat{\rho}_B \hat{M}_B^+ + \hat{M}_B^- \hat{\rho}_B \hat{M}_B^+ \right) \right)
\end{aligned}$$

There will be 6 contributions to the trace:

1. $\gamma_\perp^2 \text{Tr}_B \left(\left(\hat{M}_B^z \hat{M}_B^- + \hat{M}_B^+ \hat{M}_B^z \right) [H_B, [H_B, \hat{\rho}_B]] \right) = 0$ since $\hat{M}_B^z \hat{\rho}_B = \hat{\rho}_B \hat{M}_B^z = 0$
2. $-\gamma_\perp^2 \text{Tr}_B \left(\left[H_B, \hat{M}_B^+ \right] \left([H_B, \hat{M}_B^- \hat{\rho}_B] + \hat{M}_B^- [H_B, \hat{\rho}_B] \right) + [H_B, \hat{M}_B^-] \left([H_B, \hat{\rho}_B \hat{M}_B^+] + [H_B, \hat{\rho}_B] \hat{M}_B^+ \right) \right)$
3. $\gamma_\perp^2 \gamma_z \text{Tr}_B \left(\left\{ \hat{M}_B^z, \hat{M}_B^+ \right\} \left([H_B, \hat{M}_B^- \hat{\rho}_B] + \hat{M}_B^- [H_B, \hat{\rho}_B] \right) - \left\{ \hat{M}_B^z, \hat{M}_B^- \right\} \left([H_B, \hat{\rho}_B \hat{M}_B^+] + [H_B, \hat{\rho}_B] \hat{M}_B^+ \right) \right)$
4. $-2\gamma_\perp^2 \gamma_z \text{Tr}_B \left(-[H_B, \hat{M}_B^+] \hat{M}_B^- \hat{\rho}_B + [H_B, \hat{M}_B^-] \hat{\rho}_B \hat{M}_B^+ \right)$
5. $-2\gamma_\perp^2 \gamma_z^2 \text{Tr}_B \left(\left\{ \hat{M}_B^z, \hat{M}_B^- \right\} \hat{\rho}_B \hat{M}_B^+ + \left\{ \hat{M}_B^z, \hat{M}_B^+ \right\} \hat{M}_B^- \hat{\rho}_B \right) = 8\gamma_\perp^2 \gamma_z^2 \text{Tr}_B \left(\hat{M}_B^+ \hat{M}_B^- \hat{\rho}_B \right)$
6. $\gamma_\perp^4 \text{Tr}_B \left(\left\{ \hat{M}_B^+, \hat{M}_B^- \right\} \left(\hat{M}_B^+ \hat{M}_B^- \hat{\rho}_B + \hat{\rho}_B \hat{M}_B^+ \hat{M}_B^- + 2\hat{M}_B^- \hat{\rho}_B \hat{M}_B^+ \right) \right)$

The traces can be evaluated and disorder averaged in the Neel state to give

$$p_0^{(4)} = \underbrace{L\gamma_\perp^2 \left(\frac{W^2}{3} - 16J_z^2 - 4J_\perp^2 + 16J_\perp J_z \right)}_{\boxed{2}} + \underbrace{4L\gamma_\perp^2 \gamma_z J_\perp}_{\boxed{3}} + \underbrace{2L\gamma_\perp^2 \gamma_z (4J_z - J_\perp)}_{\boxed{4}} + \underbrace{4\gamma_\perp^2 \gamma_z^2 L}_{\boxed{5}} + \underbrace{L\gamma_\perp^4 (3L - 4)}_{\boxed{6}}. \quad (\text{D5})$$

Using the couplings for our model, the second derivative of the scalar memory kernel with an initial Neel bath state is given by

$$K^{(2)}(t=0) = - \left(\frac{W^2}{3} + \frac{3}{4} \frac{\gamma}{L} + \frac{3}{4} \frac{\gamma^2}{L} - \frac{3}{4} \frac{\gamma^2}{L^2} \right) \quad (\text{D6})$$